Electronic Supplementary Material (ESI) for Dalton Transactions.

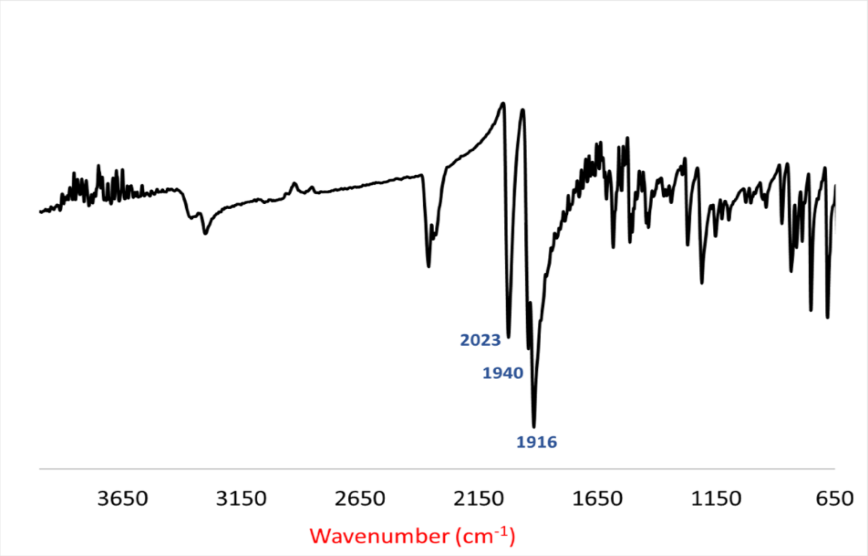
2023
1940
1916
3650
3150
2650
2150
1650
1150
650
Wavenumber (cm^{-1})

a)

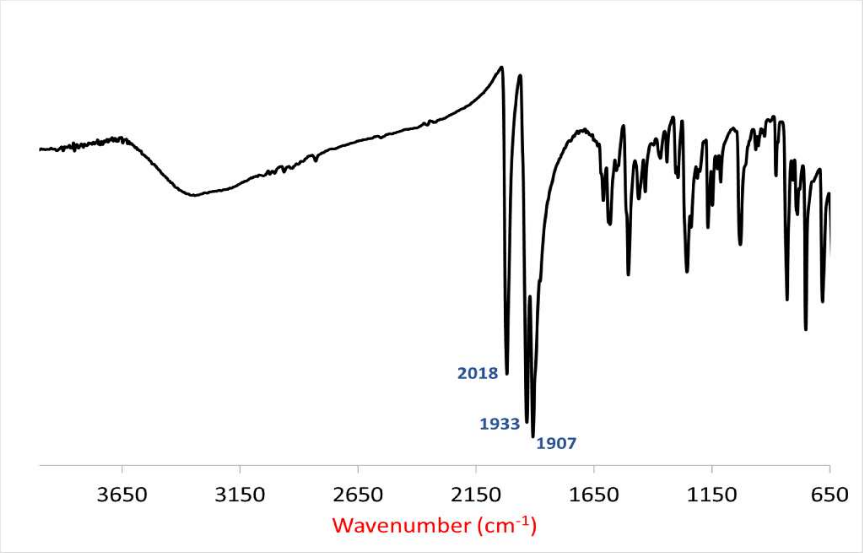
2018
1933
1907
3650
3150
2650
2150
1650
1150
650
Wavenumber (cm^{-1})

b)

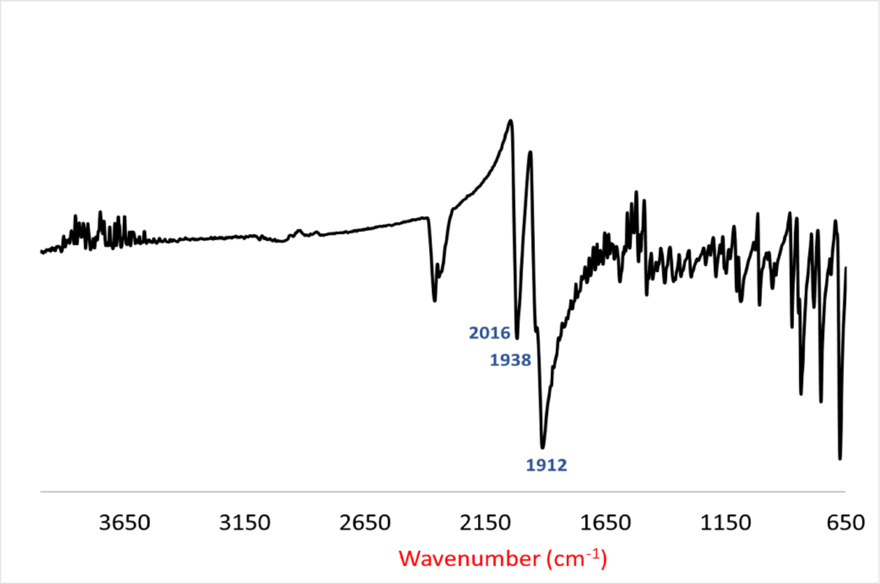
2016
1938
1912
3650
3150
2650
2150
1650
1150
650
Wavenumber (cm^{-1})

c)

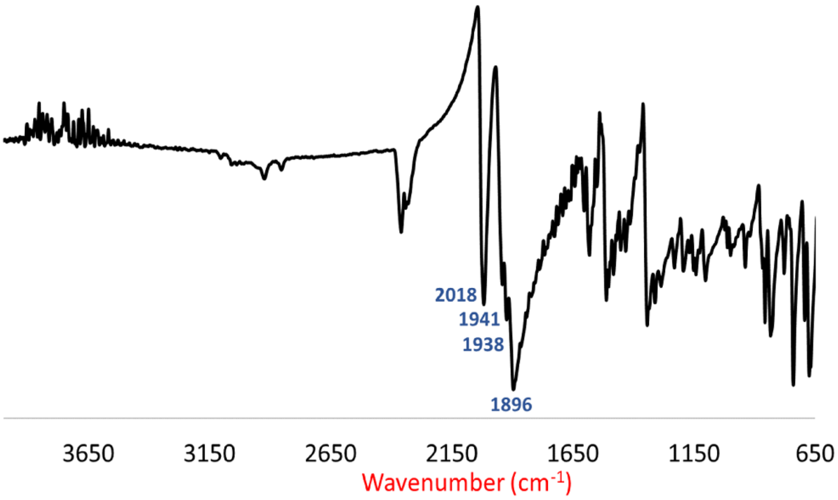
2018
1941
1938
1896
3650
3150
2650
2150
1650
1150
650
Wavenumber (cm^{-1})

d)

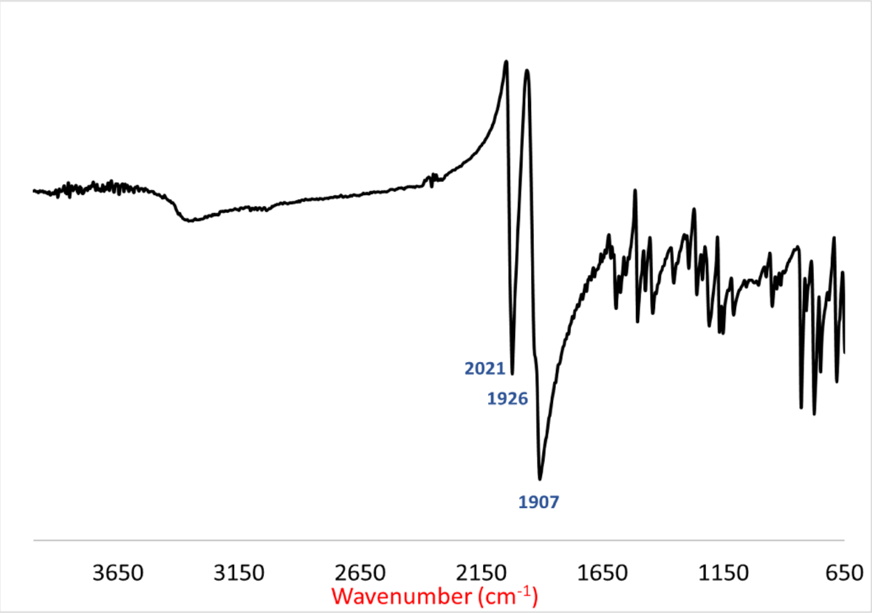
2021
1926
1907
3650
3150
2650
2150
1650
1150
650
Wavenumber (cm-1)

e)

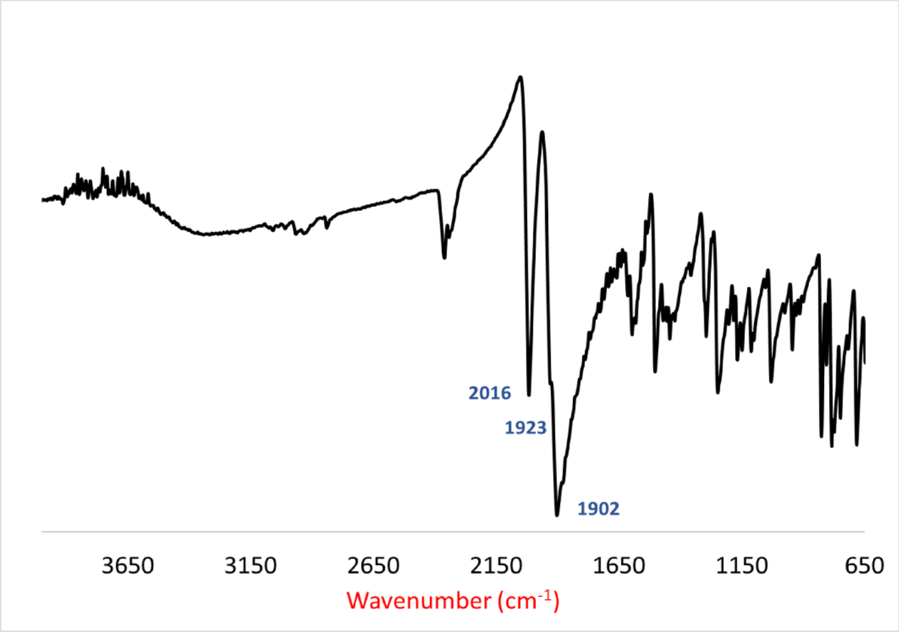
2016
1923
1902
3650
3150
2650
2150
1650
1150
650
Wavenumber (cm-1)

f)

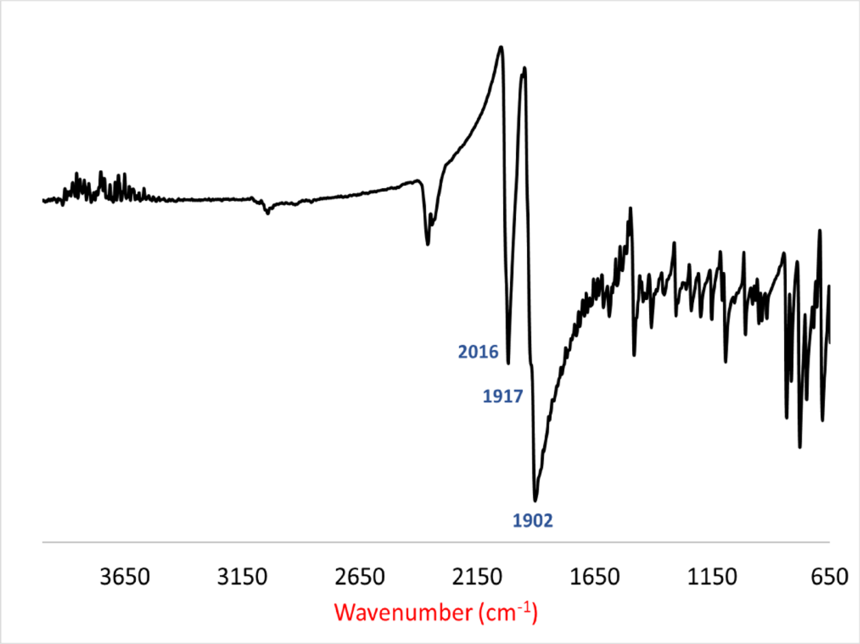

g)

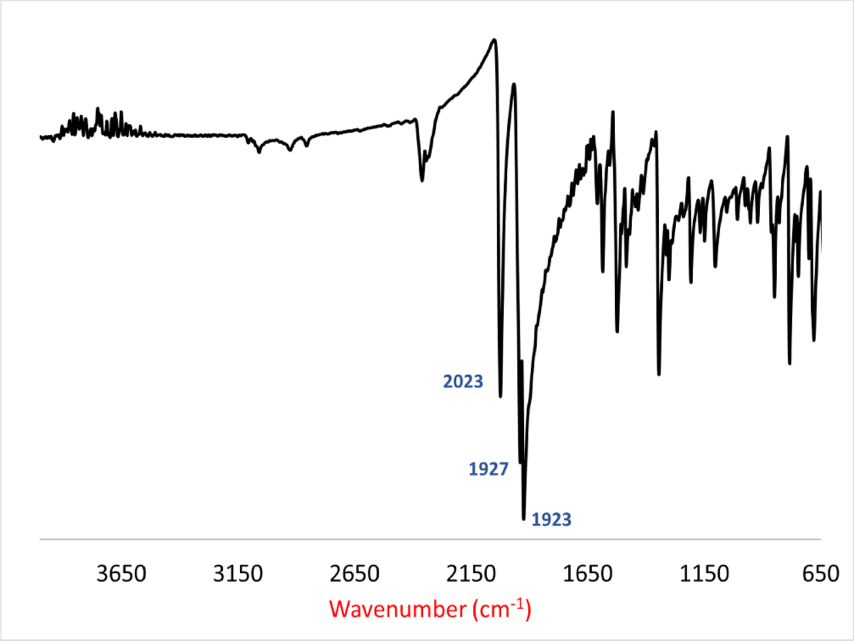

h)

Figure S1 IR spectra of tricarbonyl manganese(I) complexes a) **3**, b) **4**, c) **5**, d) **6**, e) **7**, f) **8**, g) **9**, and h) **10**.

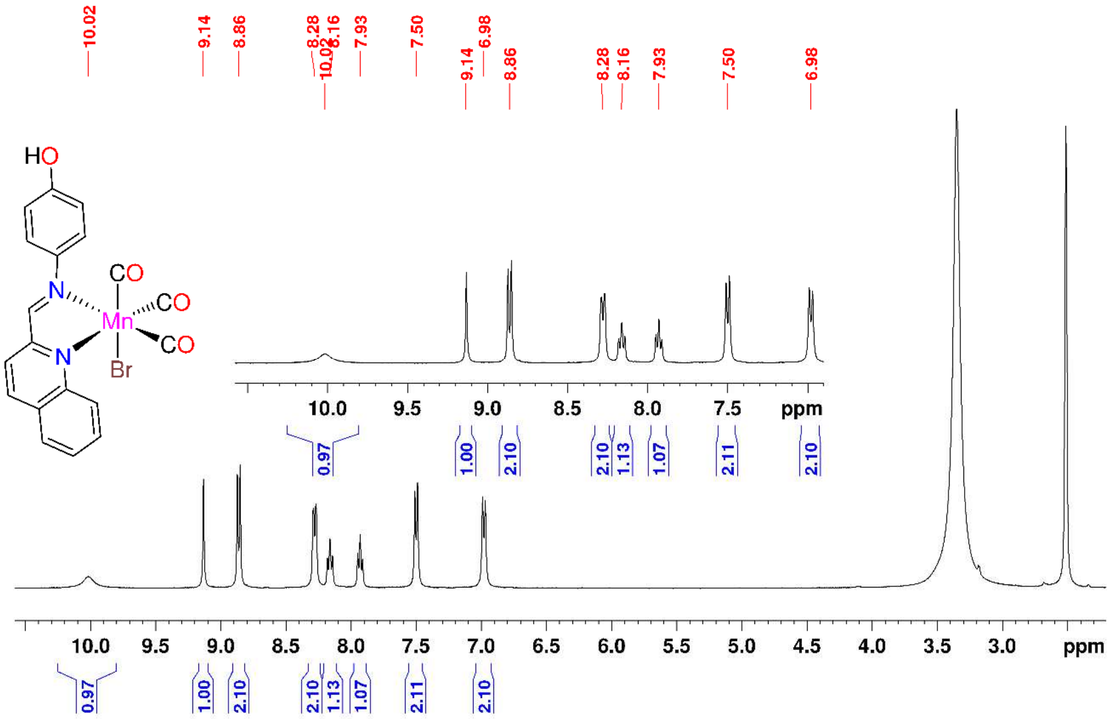
10.02
9.14
8.86
8.28
8.16
7.93
7.50
6.98
HO
N
CO
CO
CO
Mn
N
Br
10.0
9.5
9.0
8.5
8.0
7.5
7.0
6.5
6.0
5.5
5.0
4.5
4.0
3.5
3.0
ppm
0.97
1.00
2.10
2.10
1.13
1.07
2.11
2.10

a)

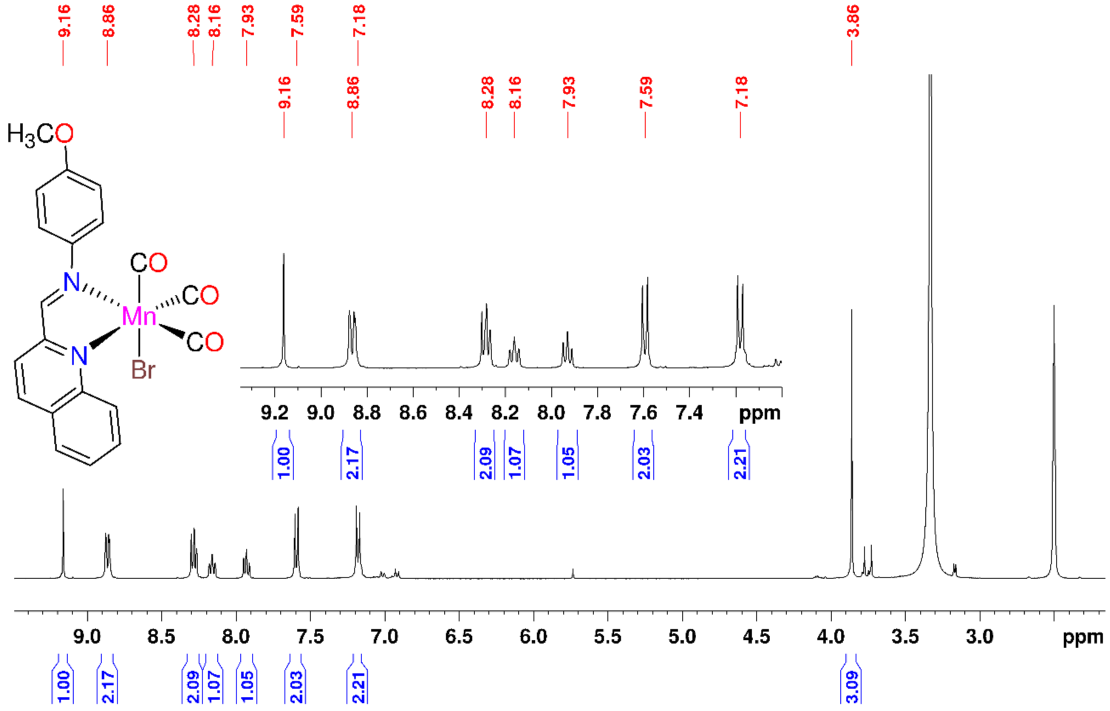
9.16
8.86
8.28
8.16
7.93
7.59
7.18
3.86
H3CO
N
CO
CO
CO
Mn
N
Br
9.2
9.0
8.8
8.6
8.4
8.2
8.0
7.8
7.6
7.4
ppm
9.0
8.5
8.0
7.5
7.0
6.5
6.0
5.5
5.0
4.5
4.0
3.5
3.0
ppm
1.00
2.17
2.09
1.07
1.05
2.03
2.21
3.09

b)

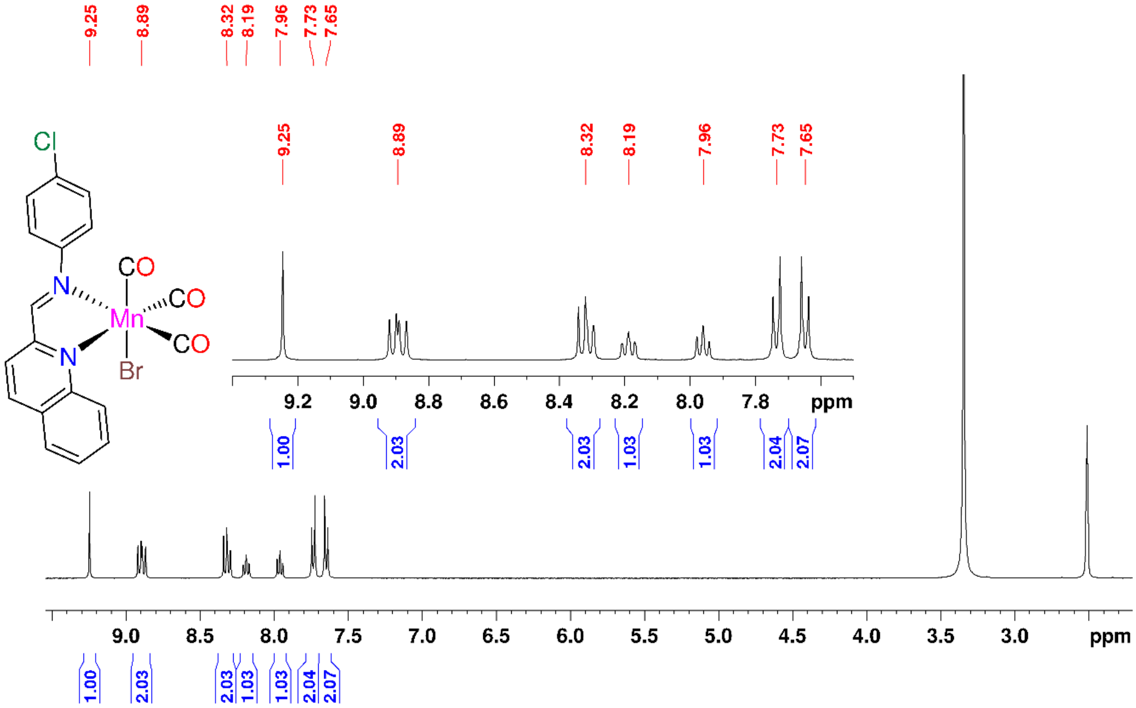
9.25
8.89
8.32
8.19
7.96
7.73
7.65
Cl
N
CO
CO
CO
Mn
N
Br
9.2
9.0
8.8
8.6
8.4
8.2
8.0
7.8
ppm
1.00
2.03
2.03
1.03
1.03
2.04
2.07
9.0
8.5
8.0
7.5
7.0
6.5
6.0
5.5
5.0
4.5
4.0
3.5
3.0
ppm

c)

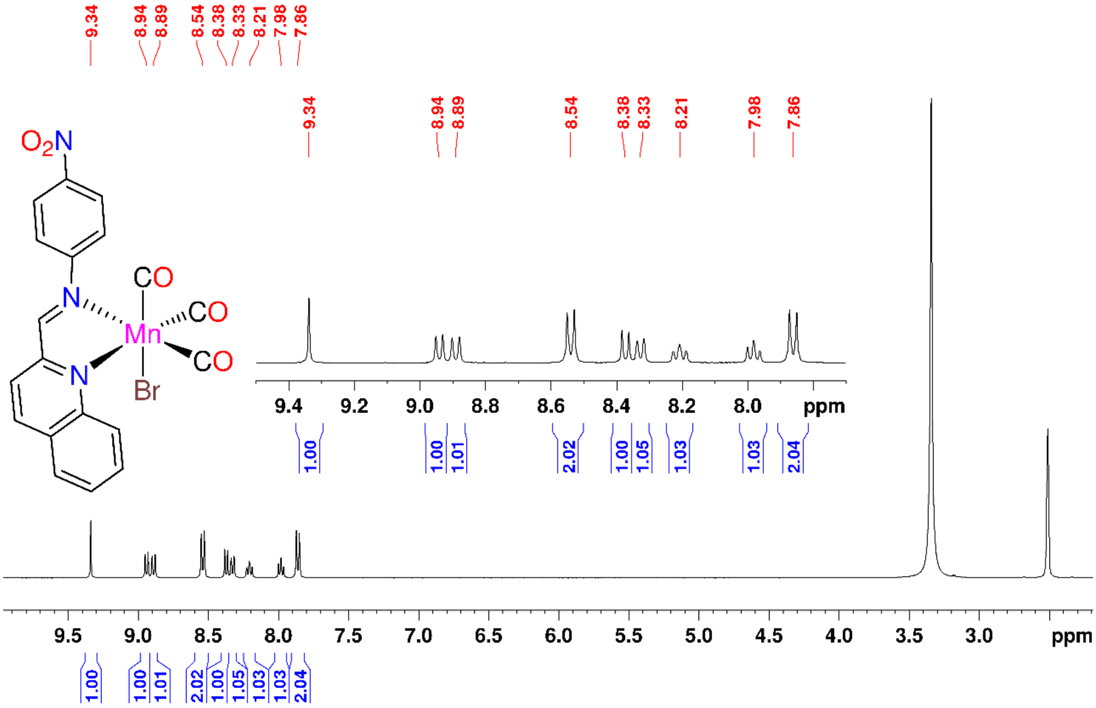
9.34
8.94
8.89
8.54
8.38
8.33
8.21
7.98
7.86
O2N
N
CO
CO
CO
Mn
N
Br
9.4
9.2
9.0
8.8
8.6
8.4
8.2
8.0
ppm
1.00
1.00
1.01
2.02
1.00
1.05
1.03
1.03
2.04
9.5
9.0
8.5
8.0
7.5
7.0
6.5
6.0
5.5
5.0
4.5
4.0
3.5
3.0
ppm

d)

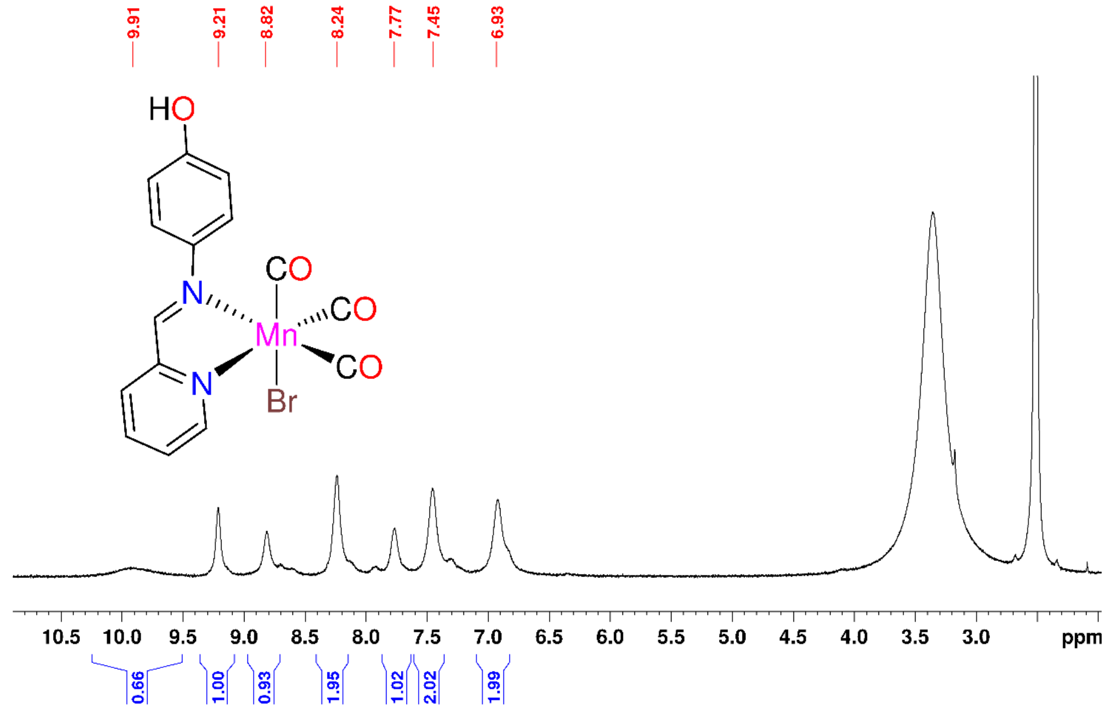
9.91
9.21
8.82
8.24
7.77
7.45
6.93
HO
N
N
CO
CO
CO
Mn
Br
10.5
10.0
9.5
9.0
8.5
8.0
7.5
7.0
6.5
6.0
5.5
5.0
4.5
4.0
3.5
3.0
ppm
0.66
1.00
0.93
1.95
1.02
2.02
1.99

e)

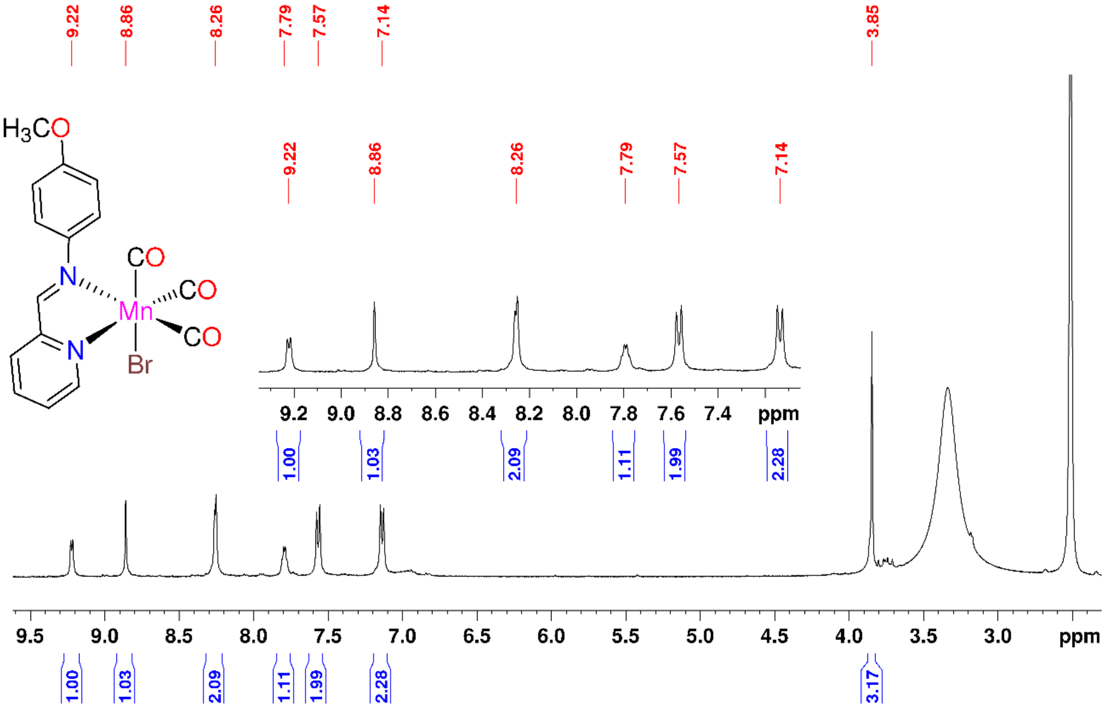
9.22
8.86
8.26
7.79
7.57
7.14
3.85
H3CO
N
N
CO
CO
CO
Mn
Br
9.22
8.86
8.26
7.79
7.57
7.14
9.2
9.0
8.8
8.6
8.4
8.2
8.0
7.8
7.6
7.4
ppm
1.00
1.03
2.09
1.11
1.99
2.28
9.5
9.0
8.5
8.0
7.5
7.0
6.5
6.0
5.5
5.0
4.5
4.0
3.5
3.0
ppm
1.00
1.03
2.09
1.11
1.99
2.28
3.17

f)

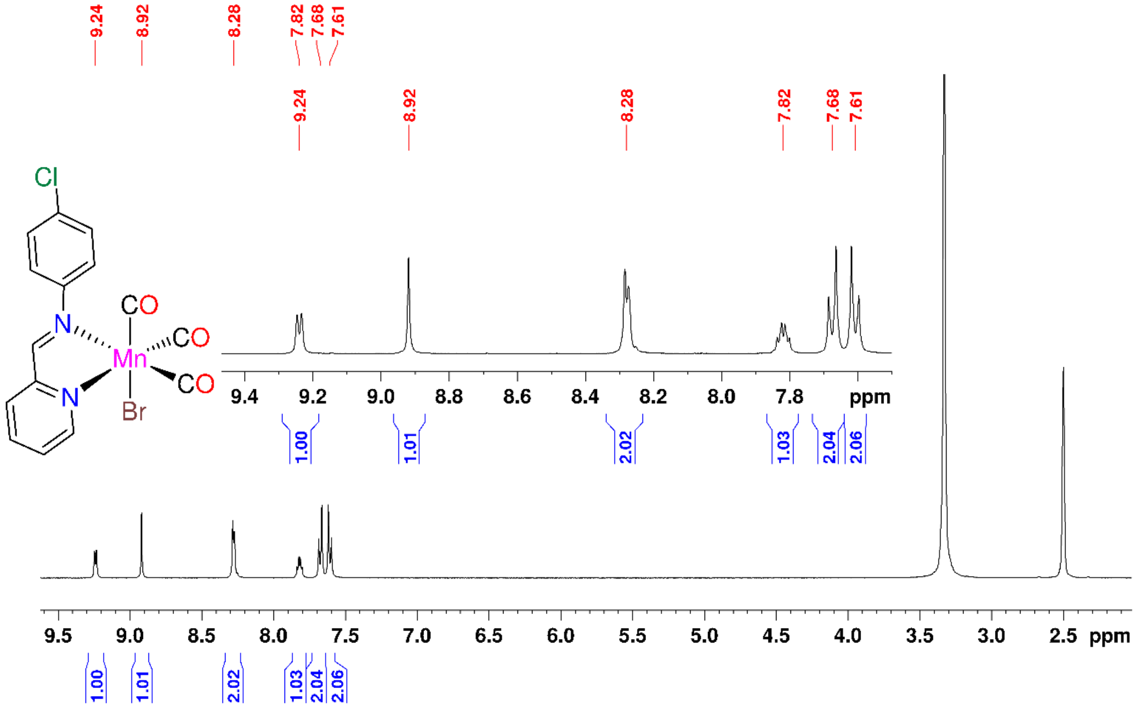

g)

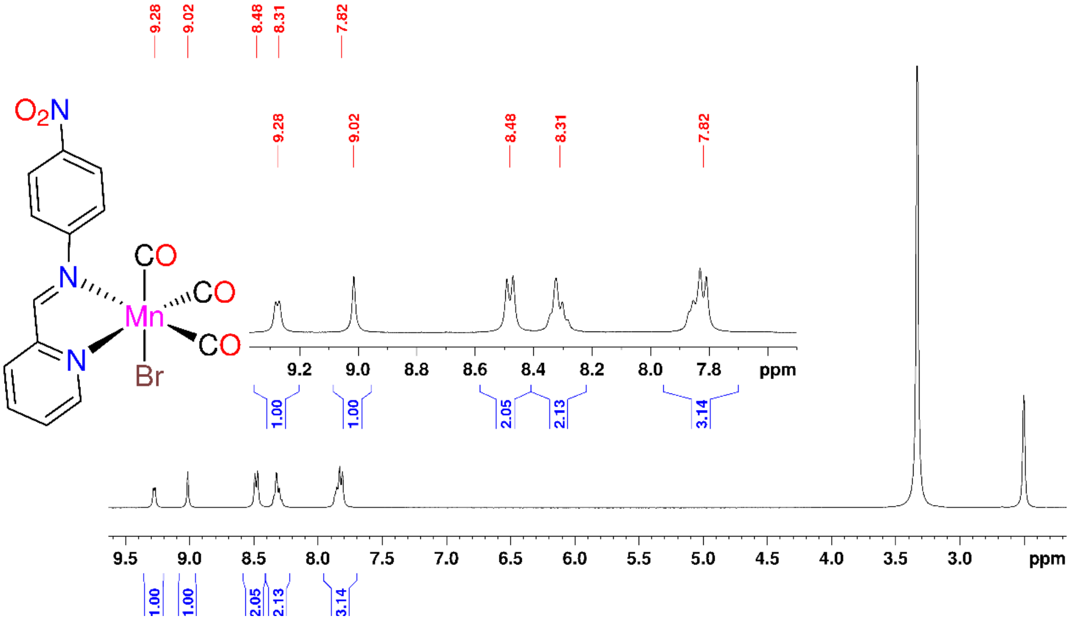

h)

Figure S2 ^{1}H NMR spectra of tricarbonyl manganese(I) complexes a) **3**, b) **4**, c) **5**, d) **6**, e) **7**, f) **8**, g) **9**, and h) **10**.

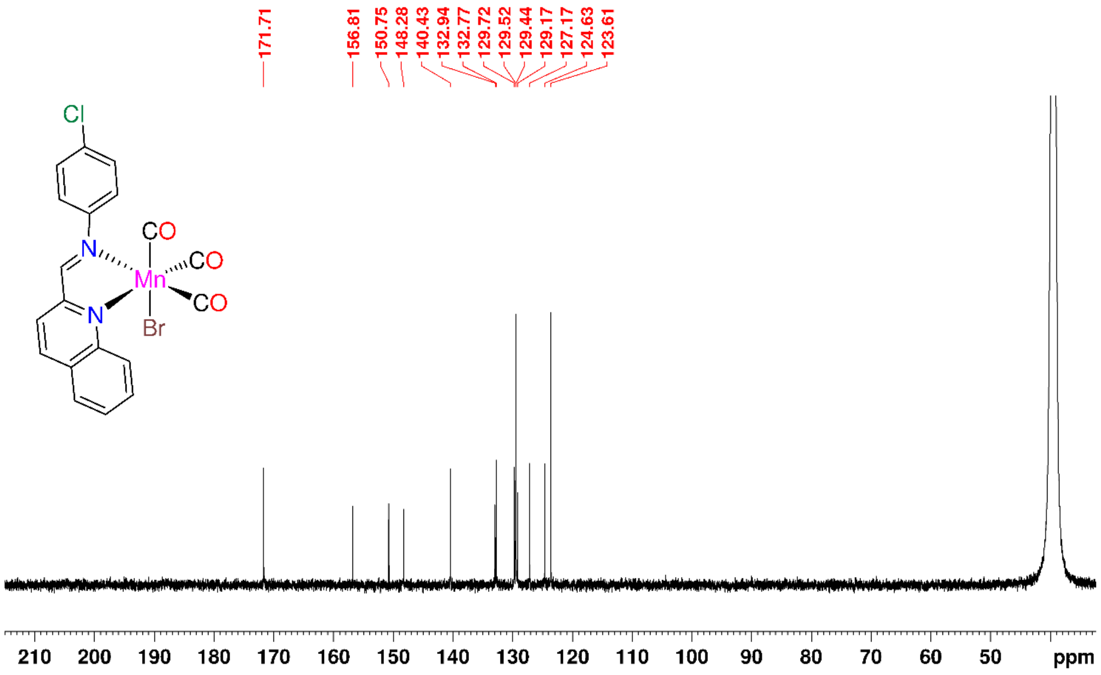
171.71
156.81
150.75
148.28
140.43
132.94
132.77
129.72
129.52
129.44
129.17
127.17
124.63
123.61
Cl
N
CO
CO
CO
Mn
N
Br
210
200
190
180
170
160
150
140
130
120
110
100
90
80
70
60
50
ppm

a)

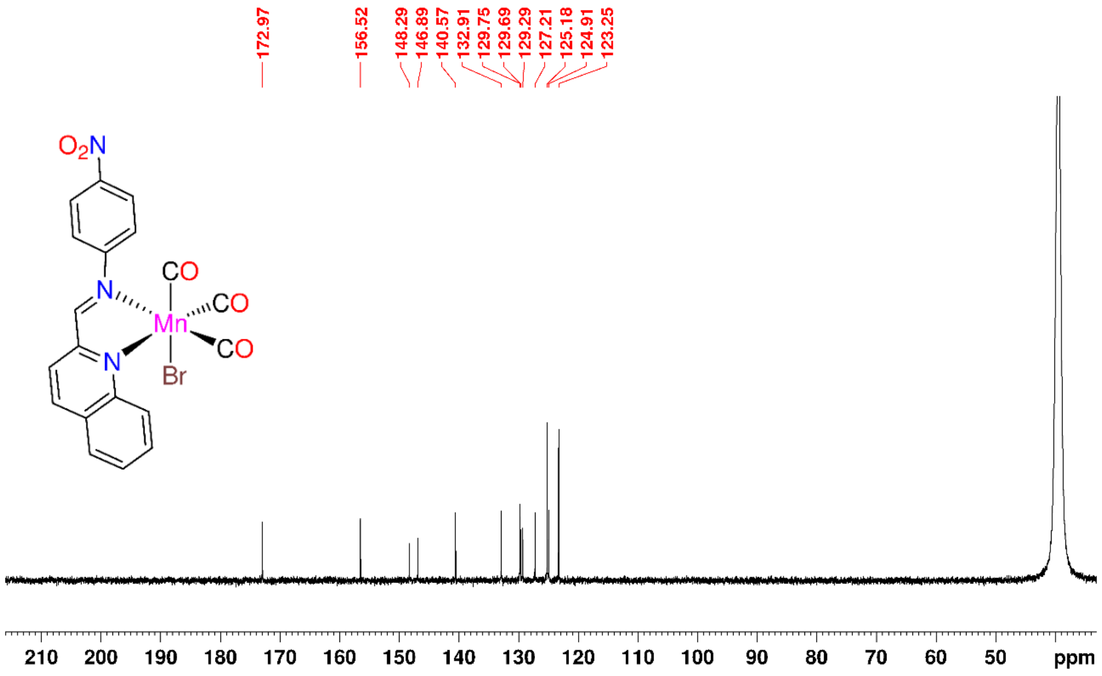
172.97
156.52
148.29
146.89
140.57
132.91
129.75
129.69
129.29
127.21
125.18
124.91
123.25
O2N
N
CO
CO
CO
Mn
N
Br
210
200
190
180
170
160
150
140
130
120
110
100
90
80
70
60
50
ppm

b)

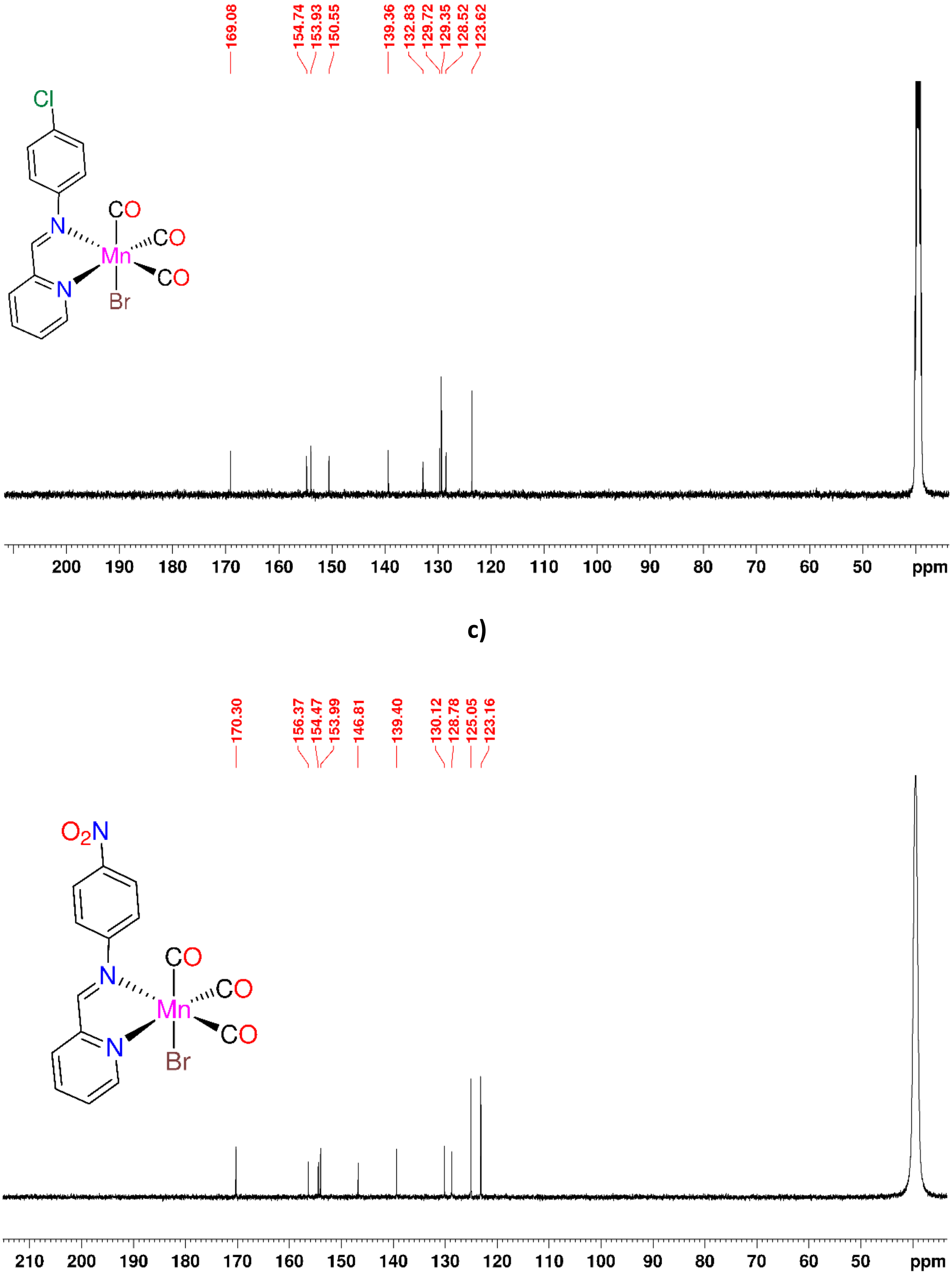

c)

d)

Figure S3 ^{13}C NMR spectra of tricarbonyl manganese(I) complexes a) **5**, b) **6**, c) **9**, and d) **10**.

Table S1 Single-crystal X-ray diffraction data and structure refinements of compounds **6**, **7**, and **9**.

Data	**6**	**7**	**9**
CCDC number	1999560	1999561	1999562
Empirical formula	$C_{19}H_{11}BrMnN_3O_5$	$C_{15}H_{10}BrMnN_2O_4$	$C_{15}H_9BrClMnN_2O_3$
Formula weight (g·mol^{-1})	496.16	417.10	435.54
Temperature (K)	100(2)	100(2)	100(2)
Radiation, λ (Å)	Cu-K$_\alpha$, 1.54184	Mo-K$_\alpha$ 0.71073	Mo-K$_\alpha$ 0.71073
Crystal size (mm^3)	0.24 × 0.20 × 0.10	0.23×0.28×0.50	0.21×0.31×0.33
Crystal color, habit	Red plate	Orange block	Red block
Crystal system	Triclinic	Monoclinic	Monoclinic
Space group	$P\bar{1}$	$P2_1/c$	$P2_1/c$
a (Å)	6.8628(2)	8.7327(17)	8.9142(19)
b (Å)	16.1907(4)	26.447(10)	26.172(7)
c (Å)	34.5806(7)	7.0400(14)	6.8978(18)
α (°)	90.292(2)	90	90
β (°)	92.660(2)	113.752(17)	109.071(7)
γ (°)	92.168(2)	90	90
Volume (Å^3)	3835.38(16)	1488.2(7)	1521.0(6)
Z	8	4	4
ρ_{calc} (g·cm^{-3})	1.719	1.862	1.902
μ (mm^{-1})	8.376	3.593	3.685
F(000)	1968	824	856
θ range (°)	2.558 – 67.066	1.540 – 28.283	2.417 – 28.280
Reflections collected	55706	23510	41145
Unique reflections	13158	3705	3773
Parameters / restraints	1046 / 0	209 / 0	208 / 0
GooF on F^2	1.059	1.041	1.045
R_1 [I>2σ(I)]	0.0981	0.0241	0.0301
wR^2 (all data)	0.2852	0.0528	0.0560
Max./min. residual electron density (e·Å^{-3})	1.962 / -1.293	0.472 / –0.401	0.507 / –0.419

The single crystal of **6** was a non-merohedral twin and had a high mosaicity with the reflections spanning several frames. This led in combination with a long c lattice parameter to unresolved reflection overlap during data reduction and, hence, to a lower data quality if compared to 7 and 9. Though residual values of the structure refinement of 6 are high, the structure solution can be considered as a proof of the conformation of the molecule.

Table S2 Selected experimental bond lengths (Å) and angles (°) of **6, 7**, and **9**.

	6 (four symmetrically non-equivalent molecules)				**7**	**9**
Mn1–Br	2.531(2)	2.5303(18)	2.522(2)	2.519(2)	2.5527(6)	2.5276(7)
Mn1–C1	1.792(12)	1.801(11)	1.801(12)	1.804(13)	1.811(2)	1.808(3)
Mn1–C2	1.801(9)	1.808(12)	1.820(11)	1.800(12)	1.822(2)	1.819(3)
Mn1–C3	1.831(13)	1.825(14)	1.817(12)	1.841(12)	1.799(2)	1.799(3)
Mn1–N1	2.082(7)	2.073(8)	2.088(8)	2.095(9)	2.040(2)	2.045(2)
Mn1–N2	2.057(9)	2.035(8)	2.041(9)	2.051(8)	2.061(1)	2.058(2)
C1–O1	1.150(13)	1.140(14)	1.134(13)	1.144(15)	1.132(3)	1.142(3)
C2–O2	1.165(11)	1.148(14)	1.133(13)	1.155(14)	1.144(2)	1.142(3)
C3–O3	1.139(13)	1.143(15)	1.158(14)	1.125(15)	1.153(2)	1.148(3)
Br–Mn1–N1	88.0(2)	90.8(2)	88.6(3)	86.0(2)	85.56(5)	87.23(6)
Br–Mn1–N2	84.6(2)	84.3(2)	86.0(2)	87.2(2)	87.39(4)	88.62(6)
Br–Mn1–C1	178.0(3)	176.7(4)	177.0(3)	176.6(4)	175.90(6)	176.50(8)
Br–Mn1–C2	88.8(3)	86.2(3)	87.3(4)	89.1(3)	88.68(6)	86.99(8)
Br–Mn1–C3	84.4(4)	83.2(4)	85.5(4)	86.4(5)	94.02(6)	89.59(7)
C1–Mn1–C2	91.6(4)	91.4(5)	91.3(5)	93.3(5)	88.90(9)	89.8(1)
C2–Mn1–C3	85.9(4)	86.4(5)	86.2(5)	84.7(6)	86.79(9)	88.5(1)
C1–Mn1–C3	93.6(5)	94.3(5)	91.8(5)	91.5(6)	89.15(9)	91.8(1)
N1–Mn1-C1	91.8(4)	91.7(4)	93.0(4)	91.9(4)	96.82(8)	95.9(1)
N1–Mn1–C2	174.8(4)	174.8(4)	173.4(4)	172.1(5)	174.24(8)	173.7(1)
N1–Mn–C3	97.9(3)	97.5(4)	98.7(4)	101.1(5)	93.95(8)	93.83(9)
N2–Mn1–C1	97.3(4)	98.3(4)	96.8(4)	94.9(4)	89.80(8)	90.4(1)
N2–Mn1–C2	96.7(4)	97.0(4)	96.2(4)	95.2(4)	100.66(8)	98.7(1)
N2–Mn1–C3	168.7(5)	166.8(4)	171.0(5)	173.6(5)	172.45(8)	172.46(9)
N1–Mn1–N2	78.9(3)	78.4(3)	78.2(3)	78.4(3)	78.75(6)	78.76(8)

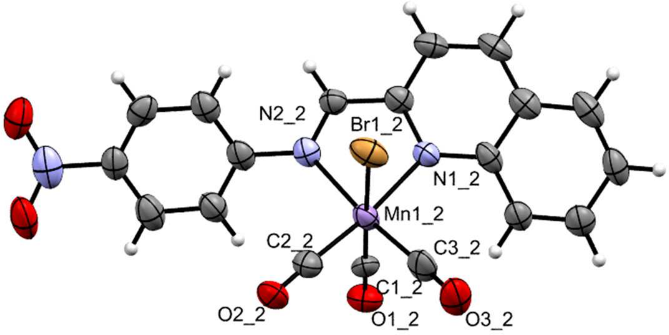

Figure S4 Molecular structure of complex **6** (thermal ellipsoids are shown at 50% probability level).

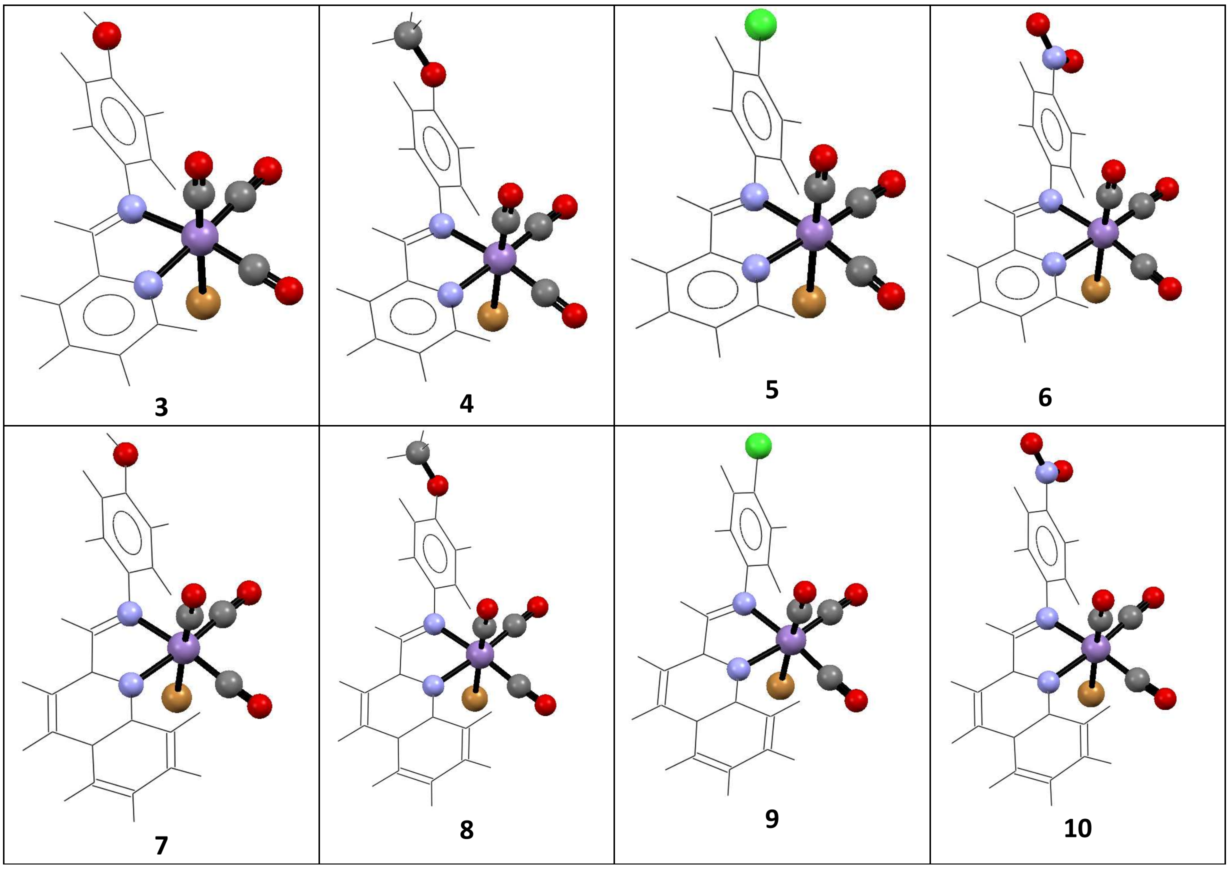

3 4 5 6

7 8 9 10

Figure S5 Local minimum structures of **3–10** calculated at B3LYP/GenECP level of theory (GenECP: LANL2DZ for Br and 6-31G(d) for the rest of elements).

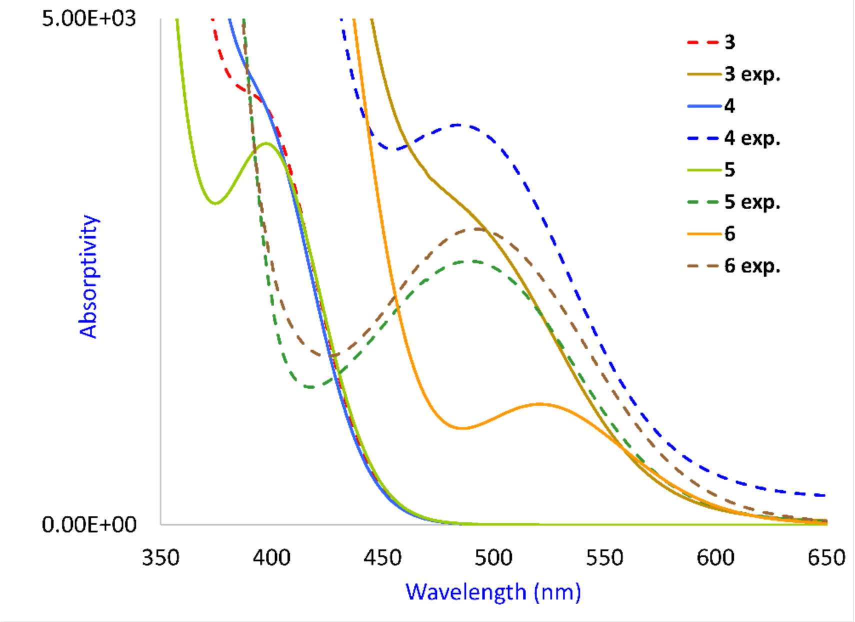

a)

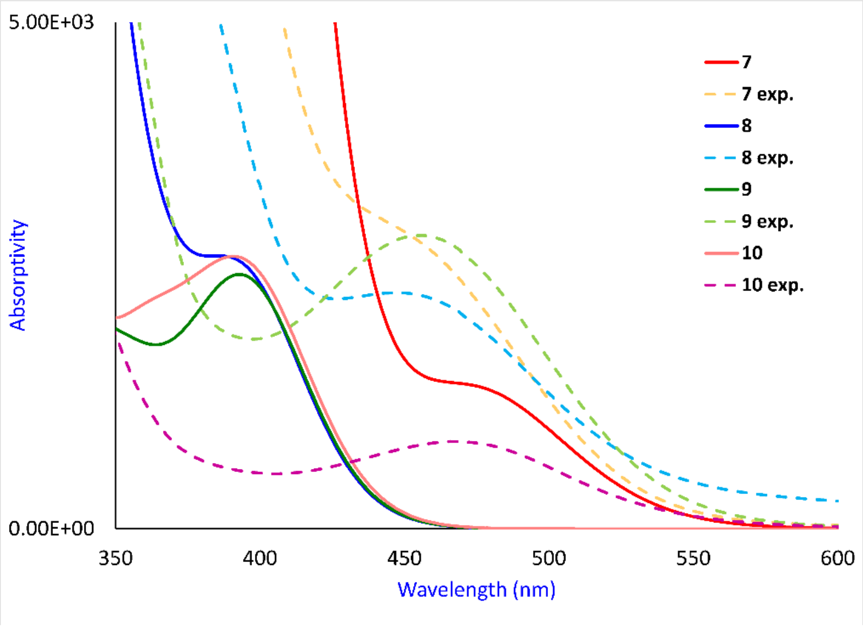

b)

Figure S6 TD-DFT calculated spectra versus experimental absorption spectra of complexes in the range of 350–600 nm a) quinoline series **3–6** and b) pyridine series **7–10**.

Table S3 Computed excitation energies (eV), electronic transition configurations and oscillator strengths (*f*) of compounds **3–10** (selected, *f* > 0.001)

Energy (cm^{-1})	Wavelength (nm)	*f*	Major contributions
• **3**			
23712	421	0.0007	HOMO→LUMO (44%)
24979	400	0.0476	HOMO–1→LUMO (51%)
26929	371	0.0045	HOMO→LUMO (33%)
28341	352	0.0017	HOMO–5→LUMO (27%)
28840	346	0.0037	HOMO–5→LUMO+3 (26%)
30168	331	0.243	HOMO–2→LUMO (55%)
30217	330	0.1201	HOMO–3→LUMO (76%)
41567	240	0.127	HOMO→LUMO+1 (36%)
• **4**			
23770	420	0.0009	HOMO→LUMO (35%)
25038	399	0.0457	HOMO–1→LUMO (41%)
26952	371	0.005	HOMO→LUMO (22%)
28368	352	0.0018	HOMO–5→LUMO (25%)
28817	347	0.0051	HOMO–5→LUMO+3 (31%)
29971	333	0.2506	HOMO–2→LUMO (47%)
30319	329	0.1519	HOMO–3→LUMO (73%)
36003	277	0.0233	HOMO–9→LUMO (34%)
41564	240	0.1124	HOMO→LUMO+1 (25%)
• **5**			
23707	421	0.0002	HOMO→LUMO (44%)
24904	401	0.0469	HOMO–1→LUMO (49%)
26858	372	0.003	HOMO→LUMO (35%)
27362	365	0.0196	HOMO–1→LUMO (23%)
30081	332	0.1133	HOMO–2→LUMO (68%)
30492	327	0.0598	HOMO–3→LUMO (44%)
33523	298	0.2113	HOMO–5→LUMO (24%)
33773	296	0.1252	HOMO–5→LUMO (23%)
40286	248	0.0228	HOMO→LUMO+2 (31%)
42728	234	0.6719	HOMO–2→LUMO+1 (37%)
• **6**[#]			
18338	545	0.0004	HOMO→LUMO (75%), HOMO→LUMO+1 (22%)
19138	522	0.0157	HOMO–1→LUMO (81%)
21831	458	0.0017	HOMO→LUMO (23%), HOMO→LUMO+1 (66%)
22411	446	0.0031	HOMO–1→LUMO+1 (74%)
23221	430	0.0079	HOMO–4→LUMO (42%), HOMO-3→LUMO (22%)
23998	416	0.0177	HOMO–2→LUMO (49%)
24252	412	0.077	HOMO–3→LUMO (46%), HOMO–2→LUMO (22%)

30224	330	0.5366	HOMO–7→LUMO (70%)
• **7**			
20552	486	0.003	HOMO→LUMO (78%)
21127	473	0.0157	HOMO–1→LUMO (80%)
24917	401	0.0904	HOMO–4→LUMO (26%), HOMO–2→LUMO (58%)
25754	388	0.0001	HOMO–5→LUMO (25%)
26264	380	0.1332	HOMO–4→LUMO (48%), HOMO–2→LUMO (32%)
26421	378	0.0645	HOMO–3→LUMO (38%)
27803	359	0.0502	HOMO–3→LUMO (40%)
32211	310	0.0159	HOMO–6→LUMO (51%), HOMO–1→LUMO+1 (27%)
36204	276	0.0223	HOMO–2→LUMO+1 (76%)
37605	265	0.0226	HOMO–8→LUMO (31%), HOMO–4→LUMO+1 (23%)
38064	262	0.0293	HOMO–2→LUMO+2 (58%)
• **8**			
24588	406	0.0012	HOMO→LUMO (21%)
25409	393	0.0324	HOMO–1→LUMO (25%)
28647	349	0.0283	HOMO→LUMO (38%)
29437	339	0.0029	HOMO–4→LUMO+3 (27%)
29706	336	0.0145	HOMO–1→LUMO (37%)
31372	318	0.2075	HOMO–2→LUMO (26%)
31524	317	0.1432	HOMO–2→LUMO (46%)
32782	305	0.0954	HOMO–3→LUMO (80%)
42097	237	0.0522	HOMO->LUMO+1 (42%)
42376	235	0.064	HOMO–1→LUMO+1 (43%)
43630	229	0.0726	HOMO–7→LUMO (56%)
• **9**			
24574	406	0.0006	HOMO→LUMO (25%)
25346	394	0.0326	HOMO–1→LUMO (27%)
32474	307	0.0986	HOMO–3→LUMO (28%), HOMO–2→LUMO (53%)
32851	304	0.0615	HOMO–4→LUMO (30%)
33560	297	0.0209	HOMO–4→LUMO (24%)
35453	282	0.2821	HOMO–5→LUMO (56%)
42162	237	0.0355	HOMO→LUMO+1 (47%)
42358	236	0.064	HOMO–1→LUMO+1 (36%)
• **10**			
24517	407	0.0003	HOMO→LUMO+1 (18%)
25230	396	0.0326	HOMO–1→LUMO (20%)
27685	361	0.0179	HOMO→LUMO (36%)
31953	312	0.0906	HOMO-2→LUMO (41%), HOMO–2→LUMO+1 (37%)
32432	308	0.0958	HOMO–4→LUMO (21%)
35223	283	0.2273	HOMO–6→LUMO (24%)
35791	279	0.1975	HOMO–6→LUMO (20%)

35919	278	0.0942	HOMO–1→LUMO (27%), HOMO–1→LUMO+1 (31%)
36801	271	0.0213	HOMO–7→LUMO (65%)
37867	264	0.0292	HOMO–5→LUMO (29%), HOMO–5→LUMO+1 (20%)
41441	241	0.0217	HOMO→LUMO+2 (20%)

[#] HOMO–2 and HOMO–3 of compound **6**.

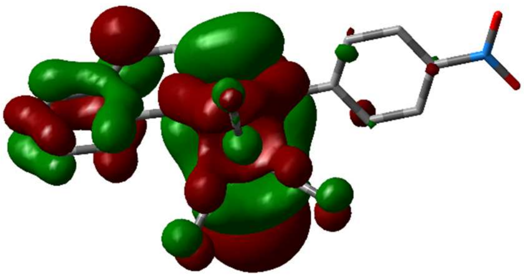

HOMO–2

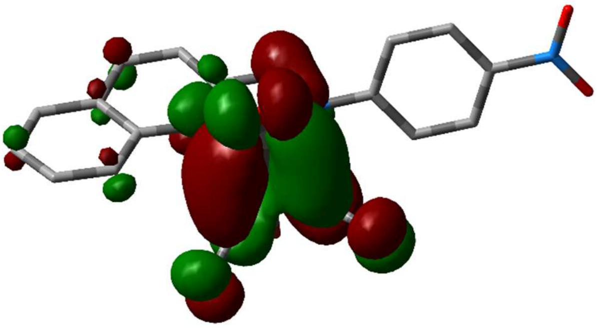

HOMO–3

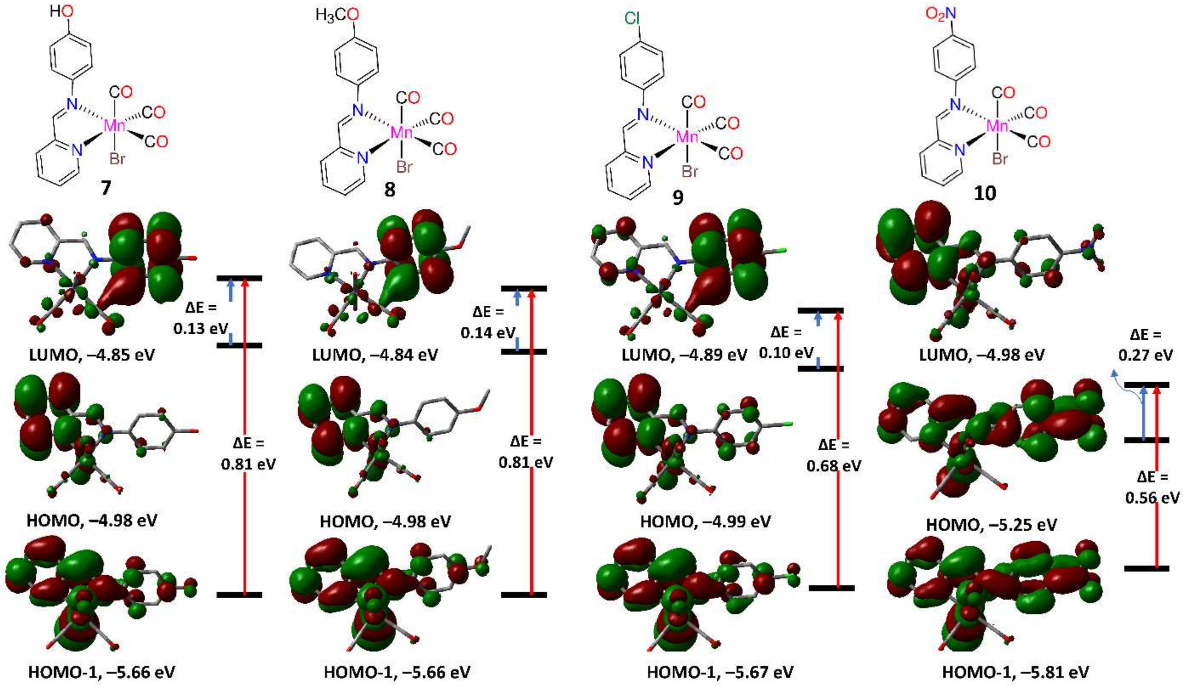

Figure S7 Selected Frontiers molecular orbitals and electronic transitions of compounds **7–10** calculated at CAM-B3LYP/LANL2DZ level of theory.

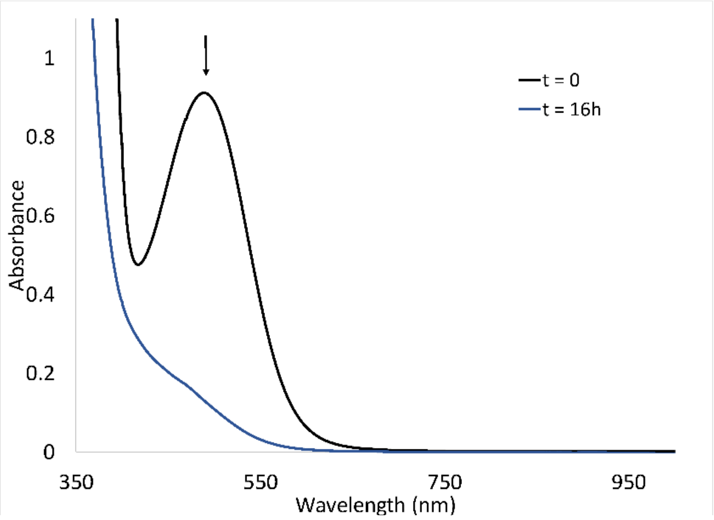

a)

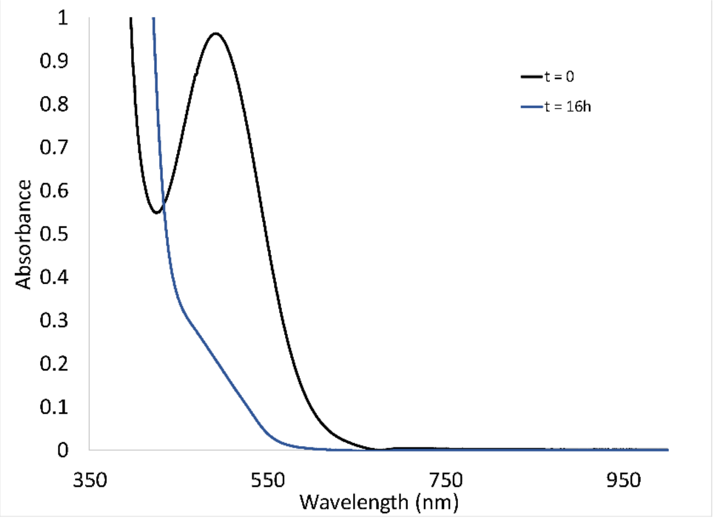

b)

Figure S8 Electronic absorption changes upon incubation of complexes a) **5** (0.35 mM) and b) **6** (0.33 mM) in DMSO in the dark for 16 h.

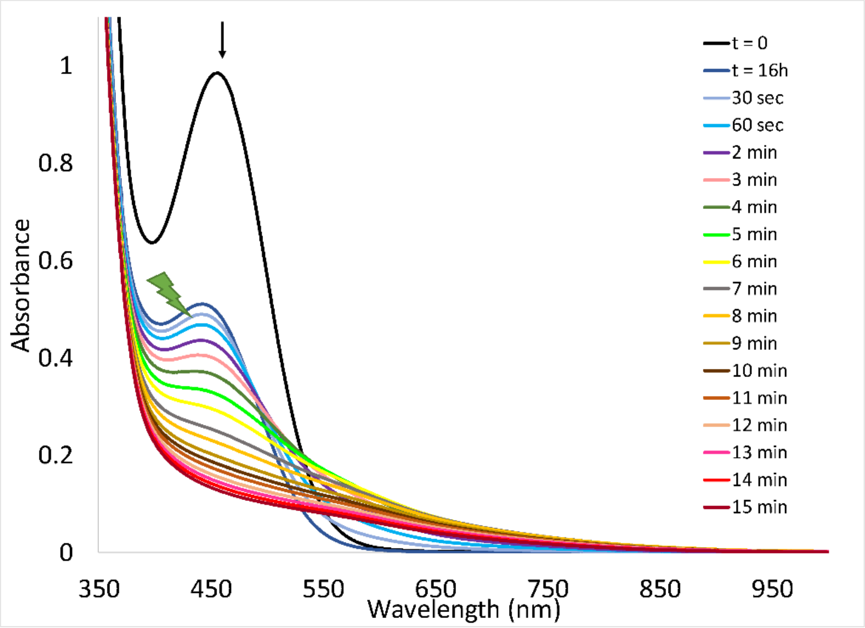

a)

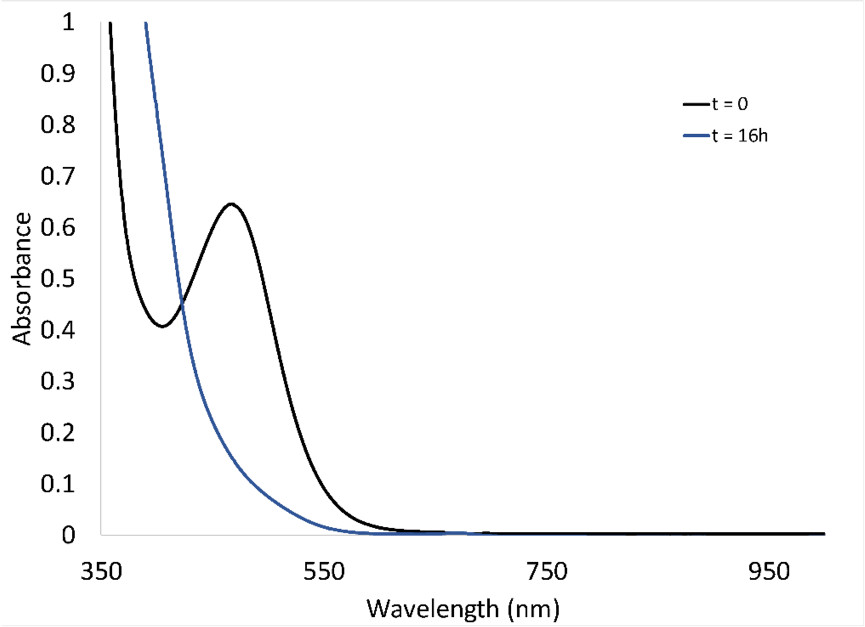

b)

Figure S9 Electronic absorption changes upon incubation of complexes a) **9** (0.34 mM) and b) **10** (0.75 mM) in DMSO in the dark for 16 h. Spectral changes upon illumination of compound **9** are shown in a).

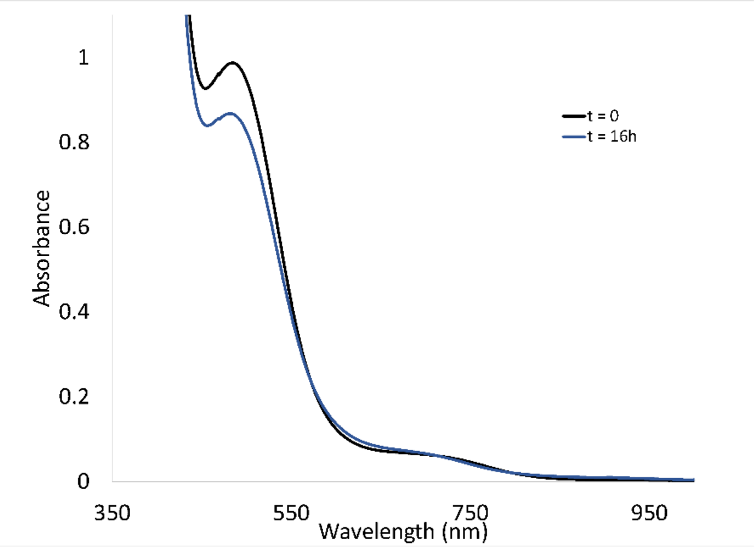

a)

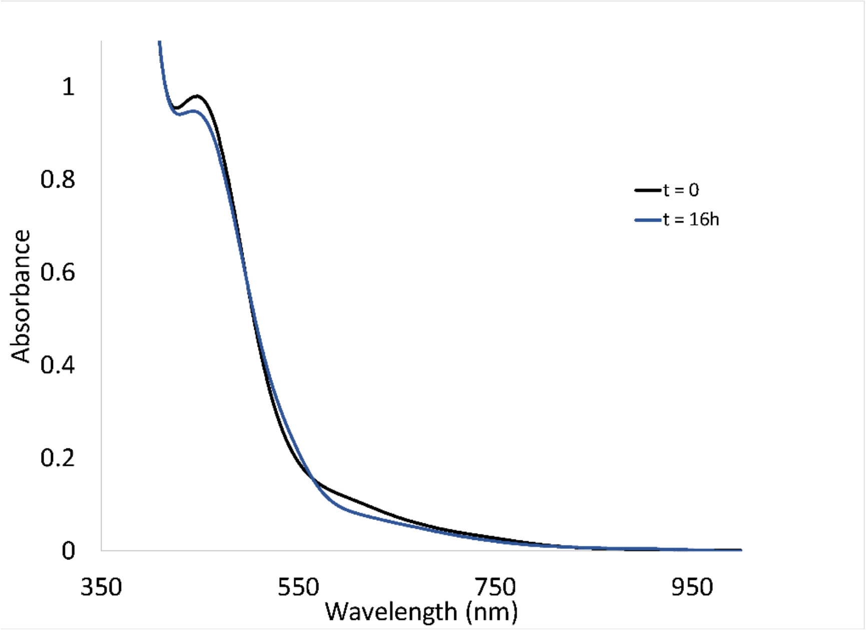

b)

Figure S10 Electronic absorption changes upon incubation of complexes a) **4** (0.25 mM) and b) **8** (0.42 mM) in DMSO in the dark for 16 h.

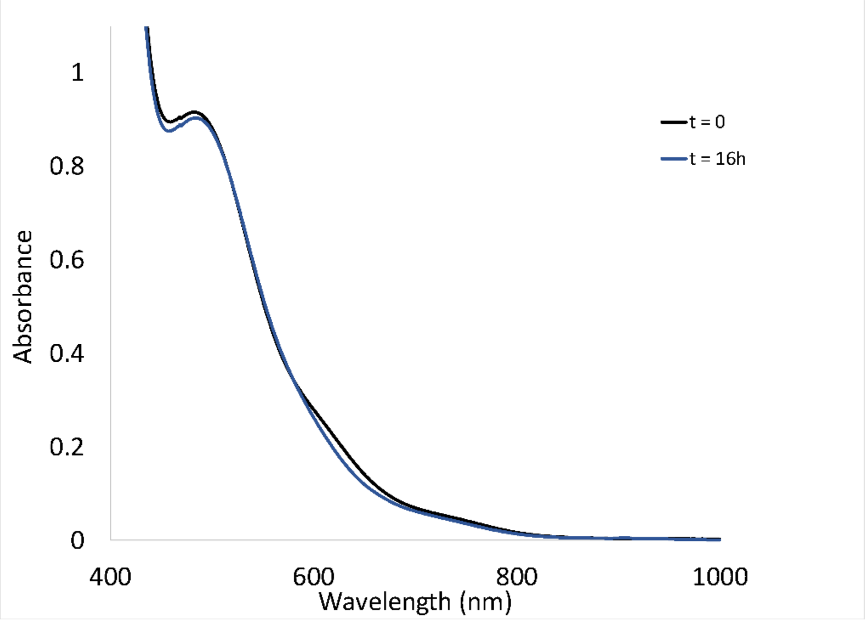

a)

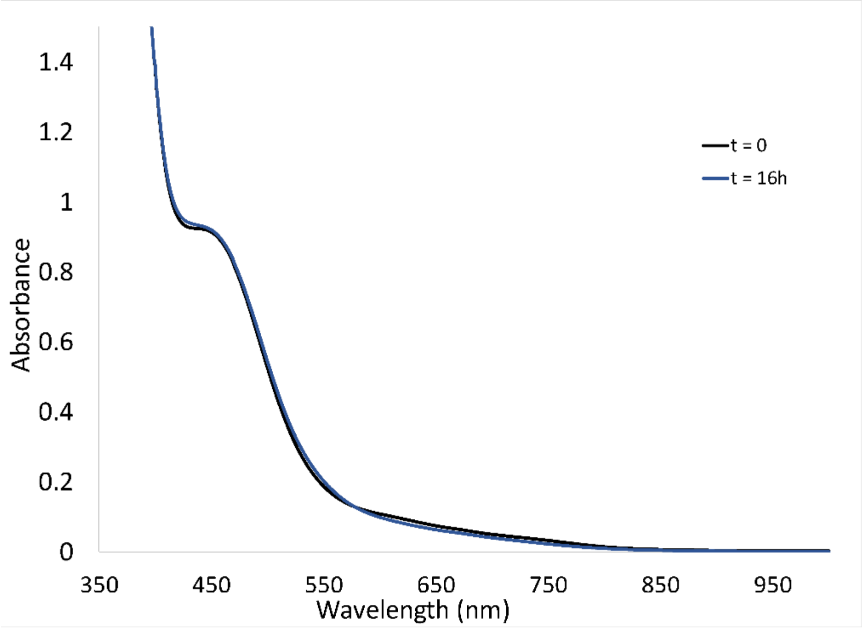

b)

Figure S11 Electronic absorption changes upon incubation of complexes a) **4** (0.2 mM) and b) **8** (0.34 mM) in DMSO in the dark in the presence of a ten-fold excess of sodium bromide for 16 h.

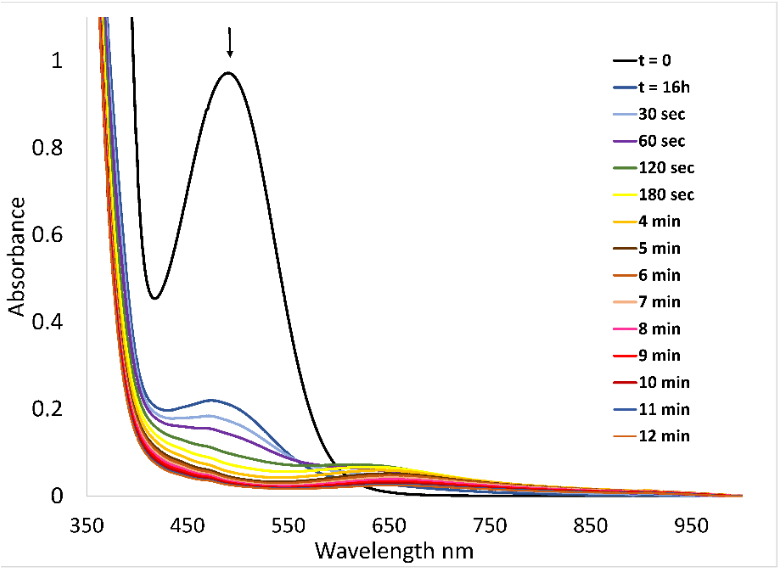
1
0.8
0.6
0.4
0.2
0
Absorbance
350
450
550
650
750
850
950
Wavelength nm
t = 0
t = 16h
30 sec
60 sec
120 sec
180 sec
4 min
5 min
6 min
7 min
8 min
9 min
10 min
11 min
12 min

a)

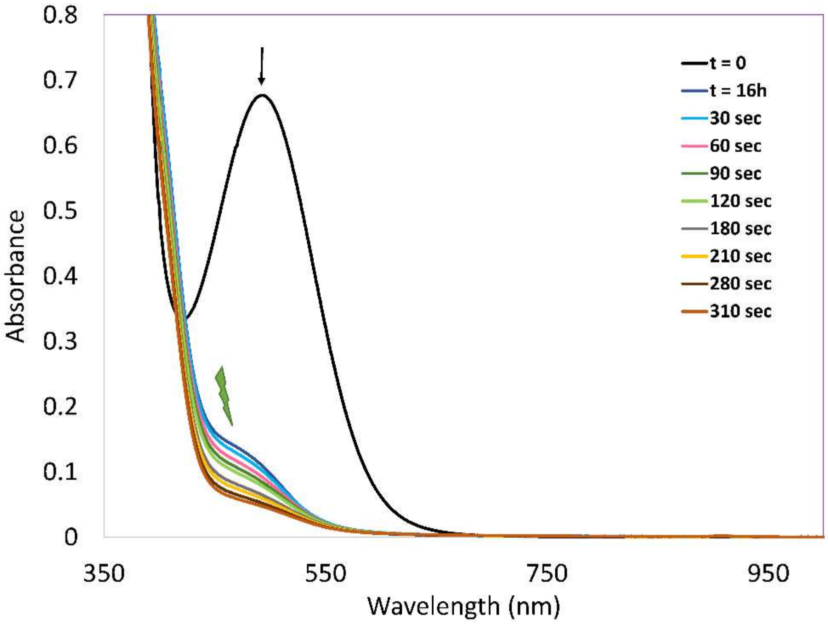
0.8
0.7
0.6
0.5
0.4
0.3
0.2
0.1
0
Absorbance
350
550
750
950
Wavelength (nm)
t = 0
t = 16h
30 sec
60 sec
90 sec
120 sec
180 sec
210 sec
280 sec
310 sec

b)

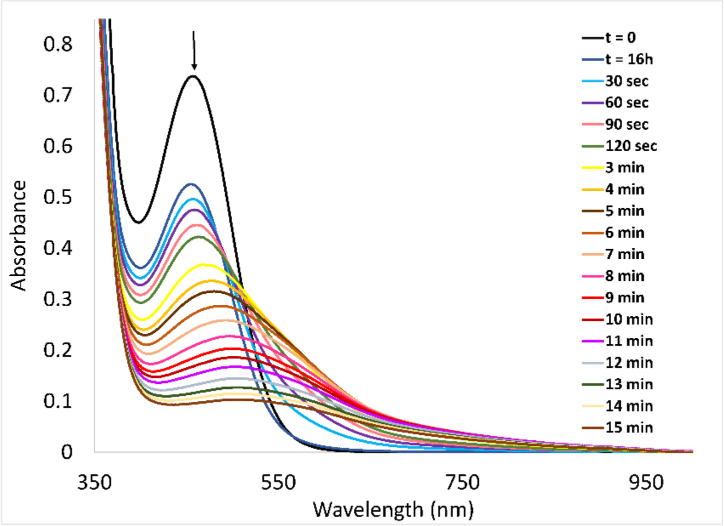

c)

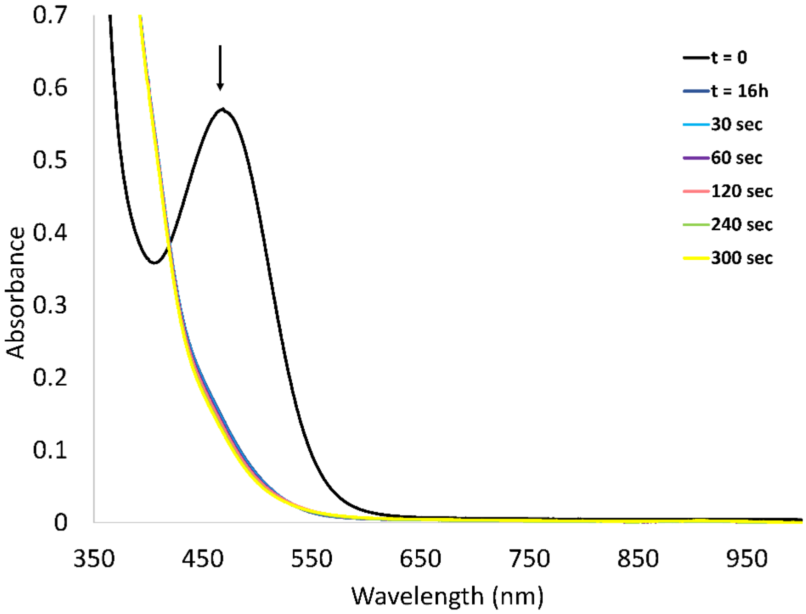

d)

Figure S12 Electronic absorption changes upon incubation of complexes a) **5** , b) 6, c) 9 and d) 10 in DMSO and NaBr salt in the dark for 16 h and spectral changes upon the illumination of at 525 nm.

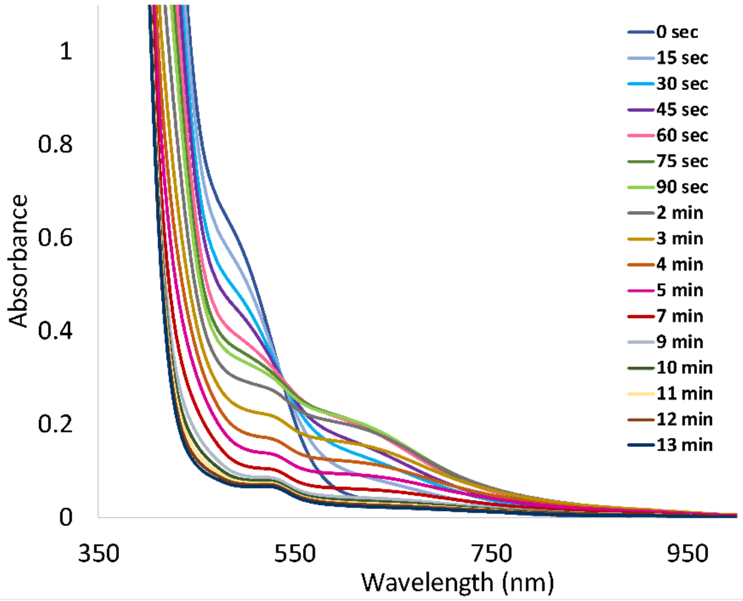

Figure S13 UV/Vis spectral changes of **3** (0.29 mM in DMSO) upon photolysis at 525 nm with increasing illumination time (0–13 min).

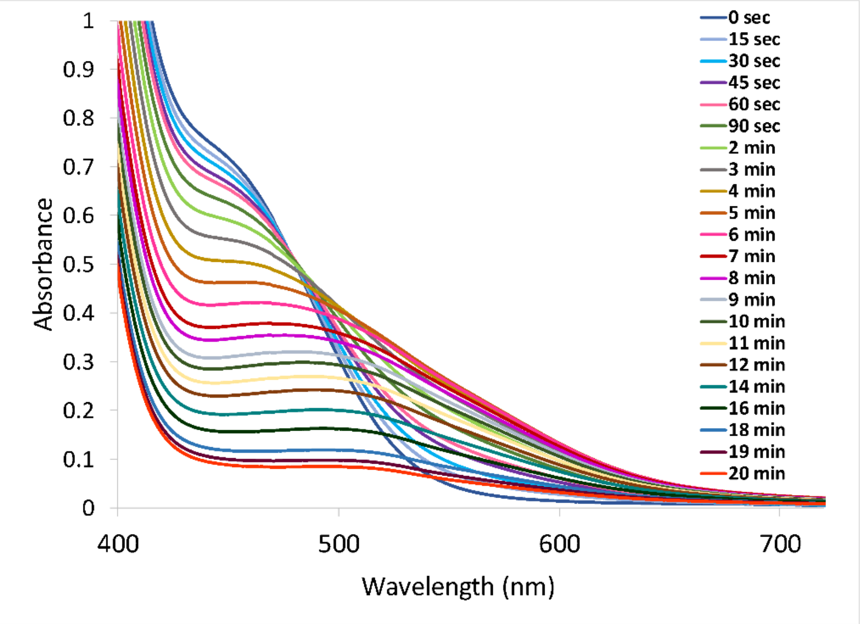

a)

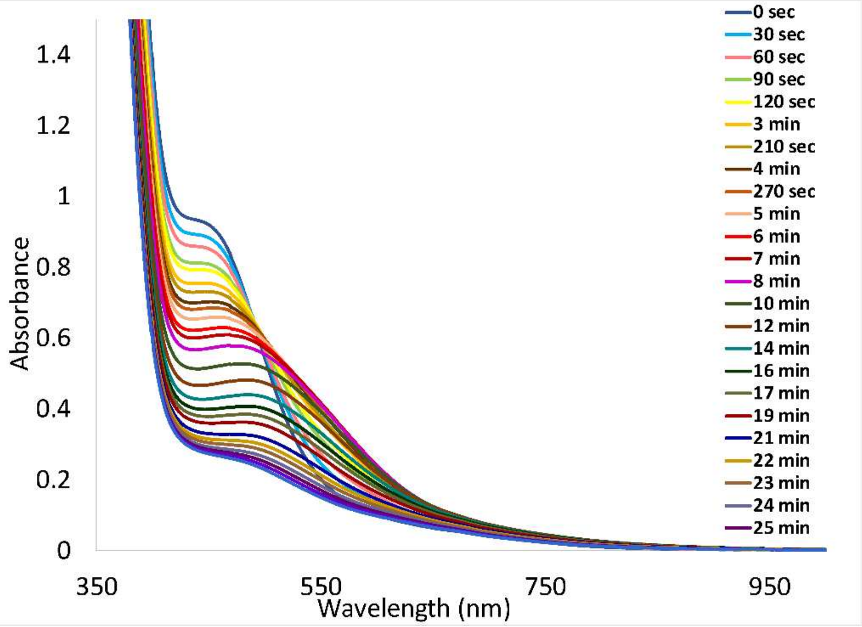

b)

Figure S14 UV/Vis spectral changes of a) **7** (0.33 mM in DMSO) and b) **8** (0.42 mM in DMSO) upon photolysis at 525 nm with increasing illumination time (0–20 min and 0–25 min respectively).

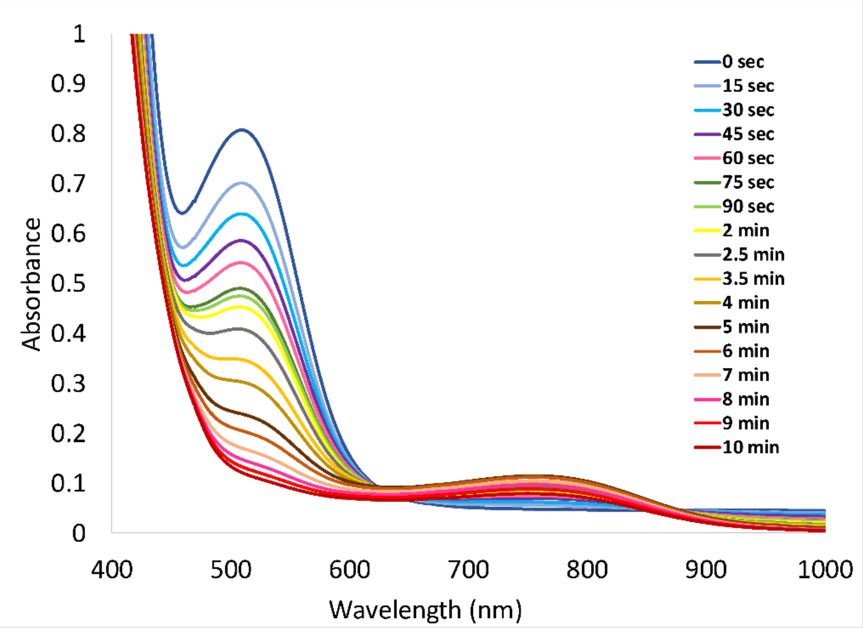

Figure S15 UV/Vis spectral changes of **3** (0.4 mM in CH_2Cl_2) upon photolysis at 525 nm with increasing illumination time (0–10 min).

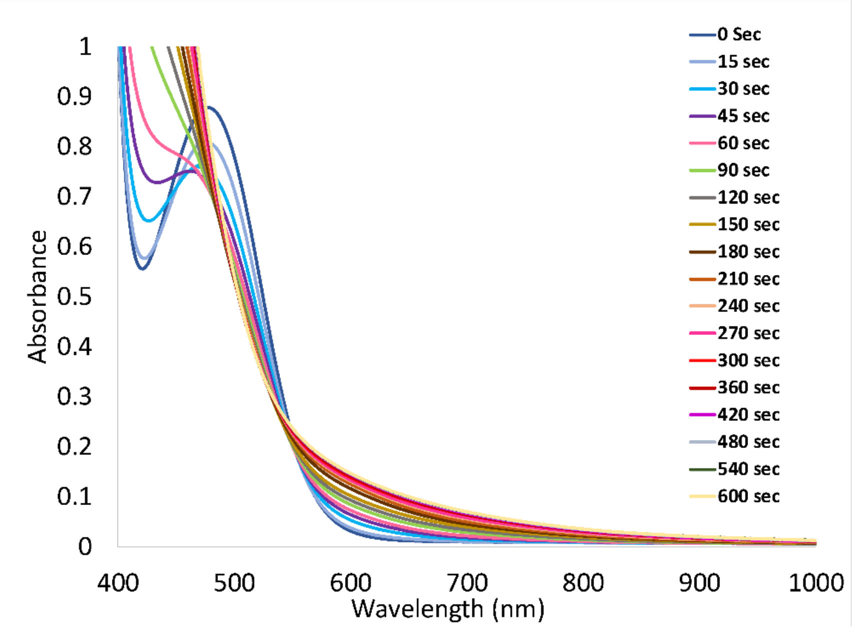

Figure S16 UV/Vis spectral changes of **7** (0.48 mM in CH_2Cl_2) upon photolysis at 525 nm with increasing illumination time (0–10 min).

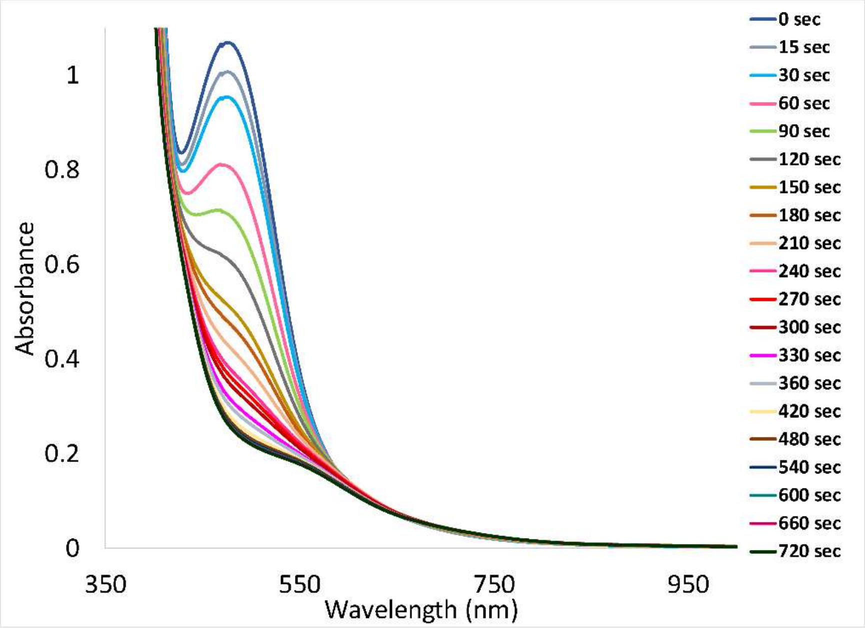

Figure S17 UV/Vis spectral changes of **8** (0.38 mM in CH_2Cl_2) upon photolysis at 525 nm with increasing illumination time (0–12 min).

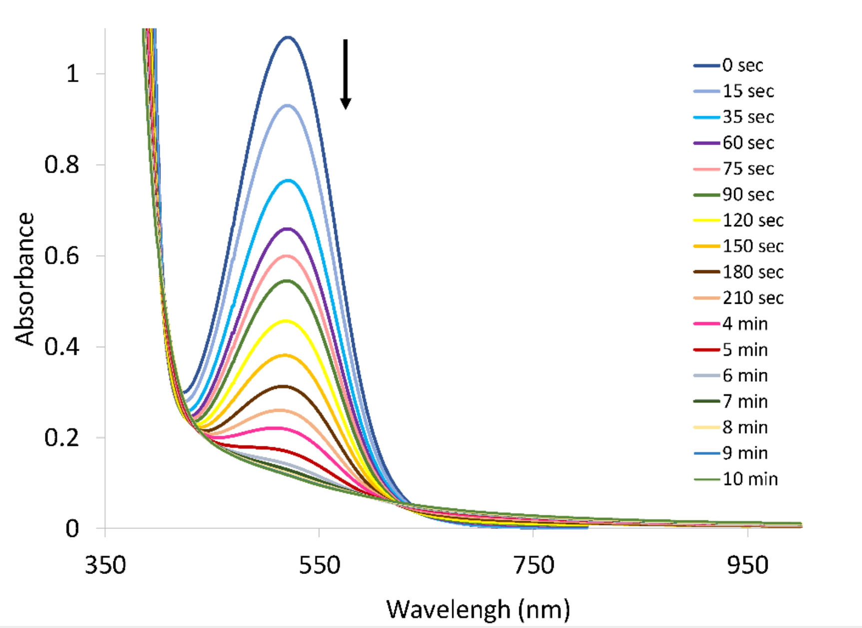

Absorbance
0
0.2
0.4
0.6
0.8
1
350
550
750
950
Wavelengh (nm)
0 sec
15 sec
35 sec
60 sec
75 sec
90 sec
120 sec
150 sec
180 sec
210 sec
4 min
5 min
6 min
7 min
8 min
9 min
10 min

a)

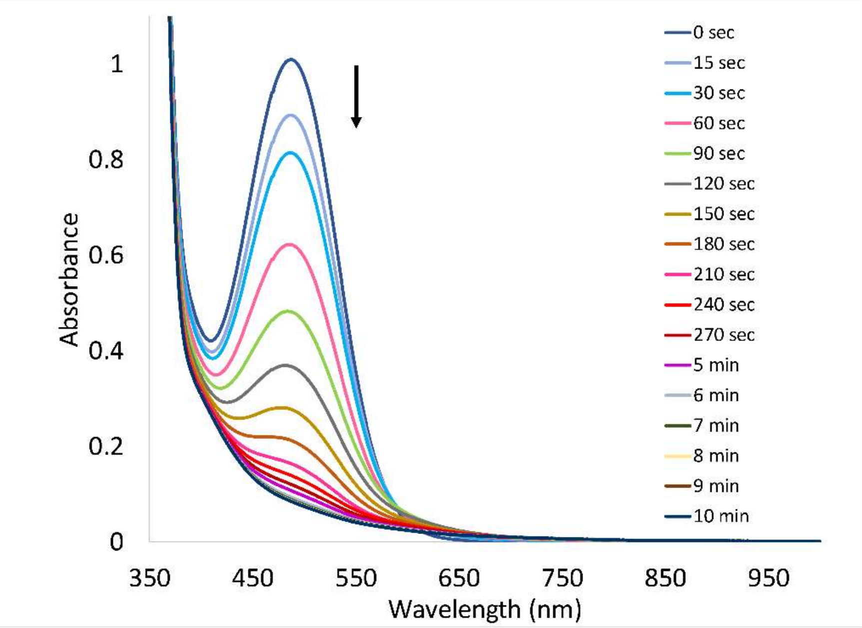

Absorbance
0
0.2
0.4
0.6
0.8
1
350
450
550
650
750
850
950
Wavelength (nm)
0 sec
15 sec
30 sec
60 sec
90 sec
120 sec
150 sec
180 sec
210 sec
240 sec
270 sec
5 min
6 min
7 min
8 min
9 min
10 min

b)

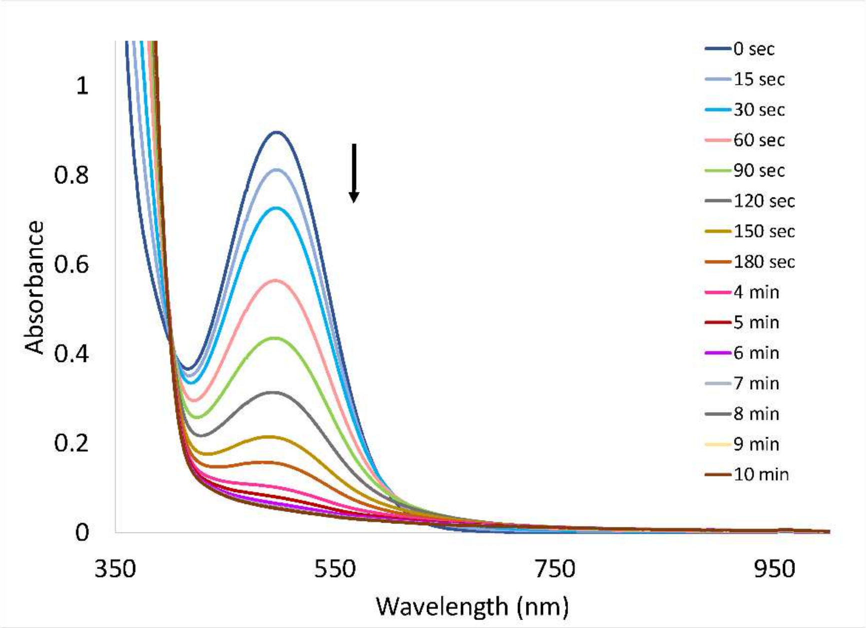

c)

Figure S18 UV/Vis spectral changes of **a) 5** (0.3 mM in CH_2Cl_2), **b) 9** (0.38 mM in CH_2Cl_2) and **c) 10** (0.37 mM in CH_2Cl_2) upon photolysis at 525 nm with increasing illumination time (0–10 min).

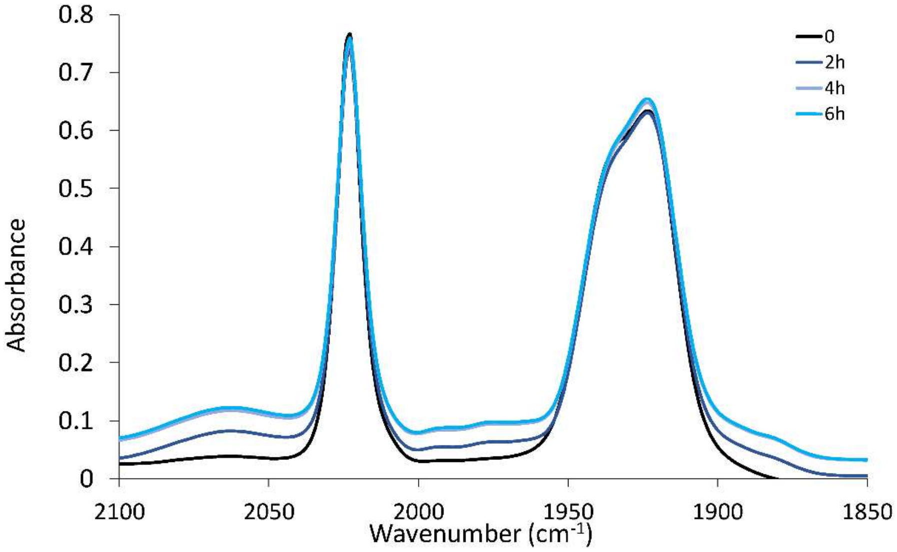
0.8
0.7
0.6
0.5
0.4
0.3
0.2
0.1
0
Absorbance
2100
2050
2000
1950
1900
1850
Wavenumber (cm^{-1})
0
2h
4h
6h

a)

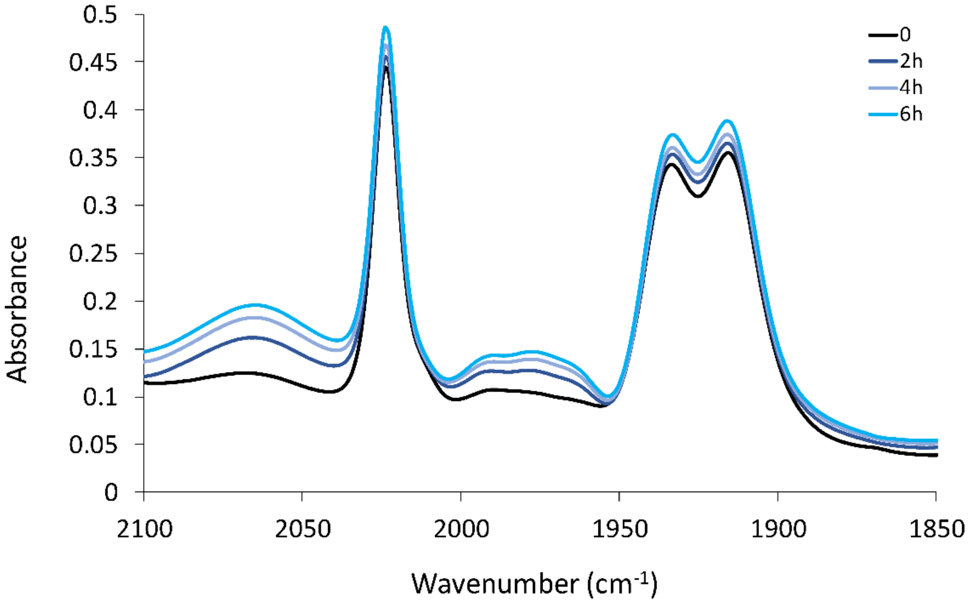
0.5
0.45
0.4
0.35
0.3
0.25
0.2
0.15
0.1
0.05
0
Absorbance
2100
2050
2000
1950
1900
1850
Wavenumber (cm^{-1})
0
2h
4h
6h

b)

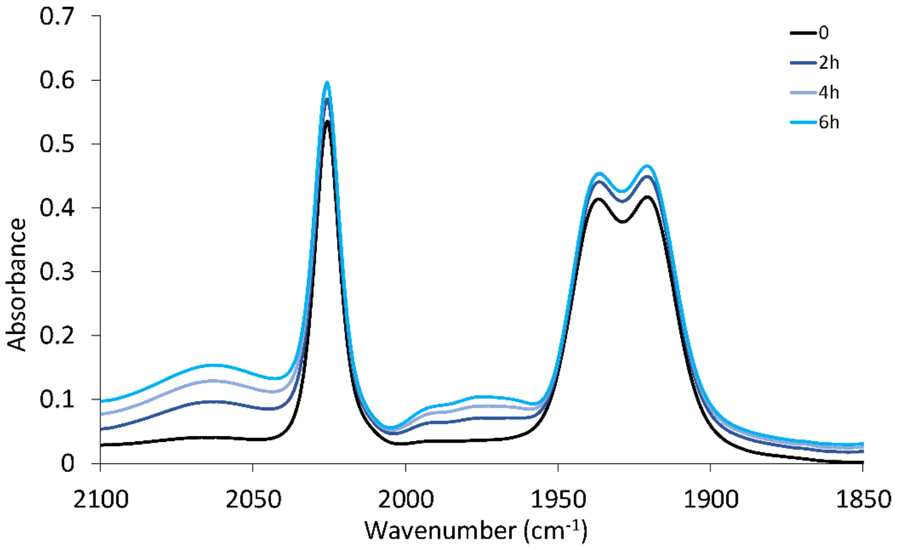

c)

Figure S19 IR spectral changes upon incubation of complexes (8 mM) a) **4**, b) **8** and c) **10** in DMSO in the dark for 6 h.

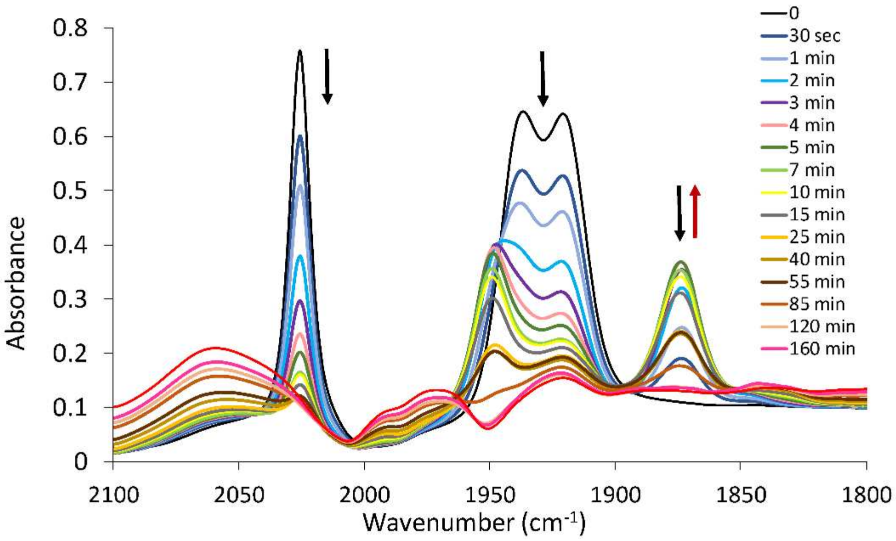

Figure S20 Time dependent changes in the IR spectra of DMSO solution of compound **10** (8 mM) upon photolysis at 525 nm with increasing illumination time (0–160 min).

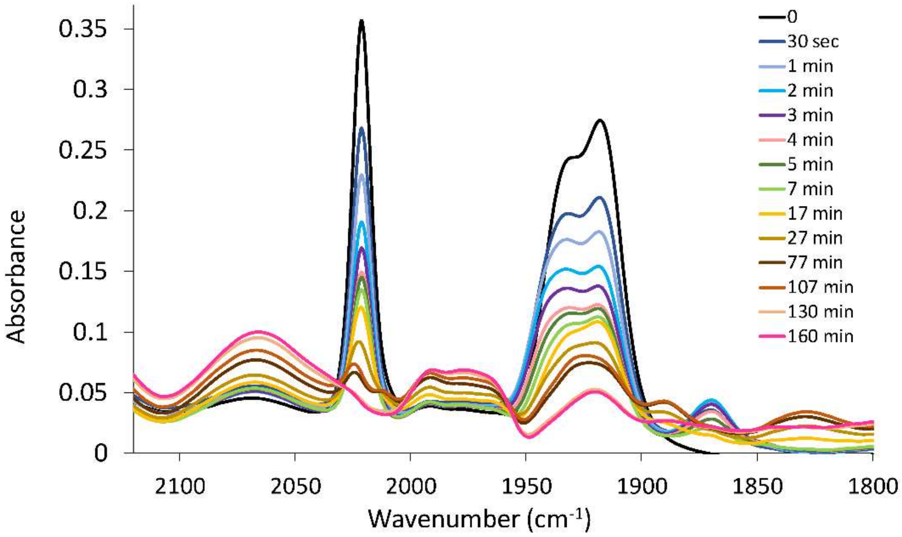

Figure S21 Time dependent changes in the IR spectra of DMSO solution of compound **4** (8 mM) upon photolysis at 525 nm with increasing illumination time (0–160 min).

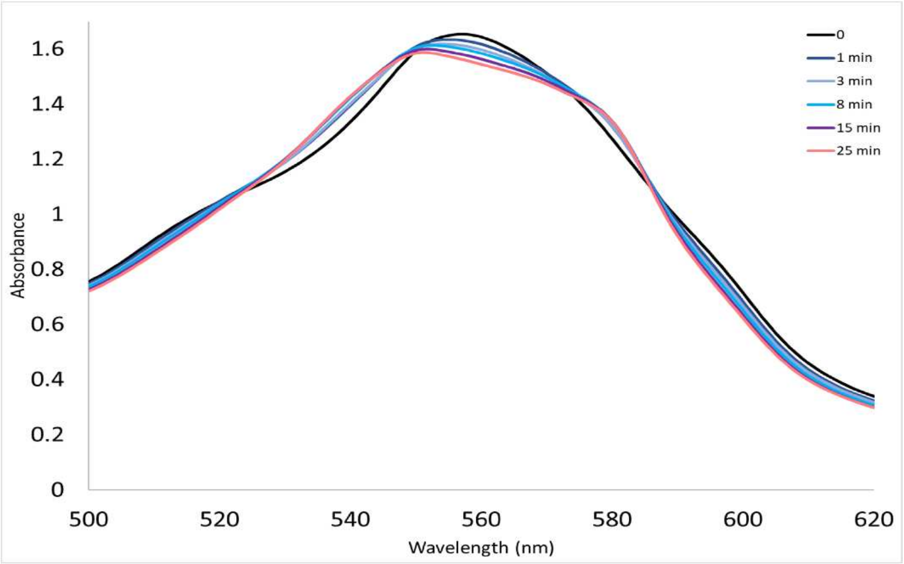

a)

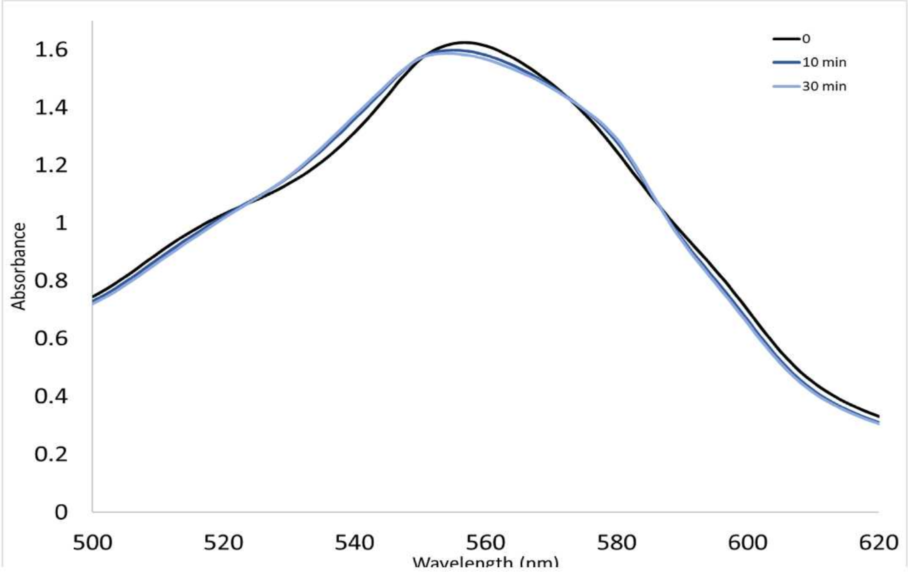

b)

Figure S22 UV/Vis spectral changes in the Q-band region of myoglobin (60 **μ**M in 0.1 PBS at pH 7.4) with sodium dithionite (10 mM) and complex **4** (40 **μ**M) under a dinitrogen atmosphere upon photolysis at a) 468 nm and b) 525 nm.

Hammett plots

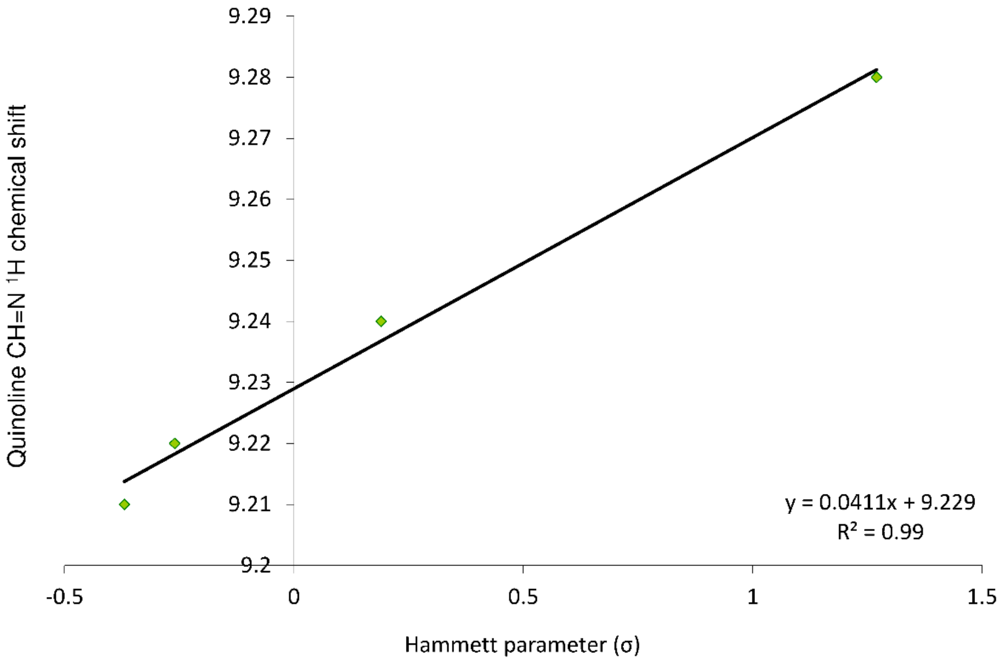

a)

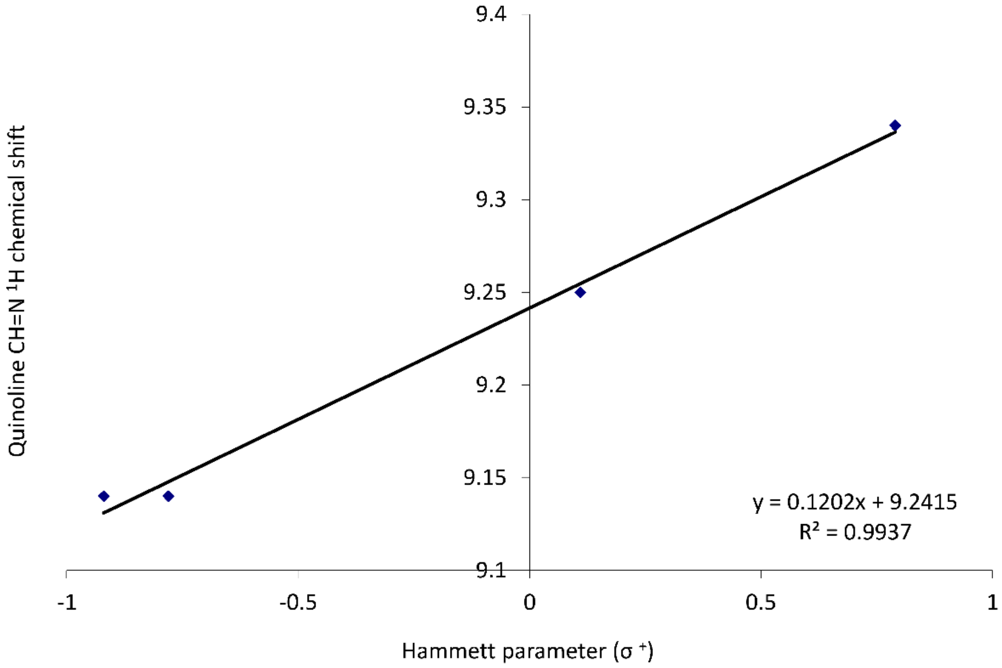

b)

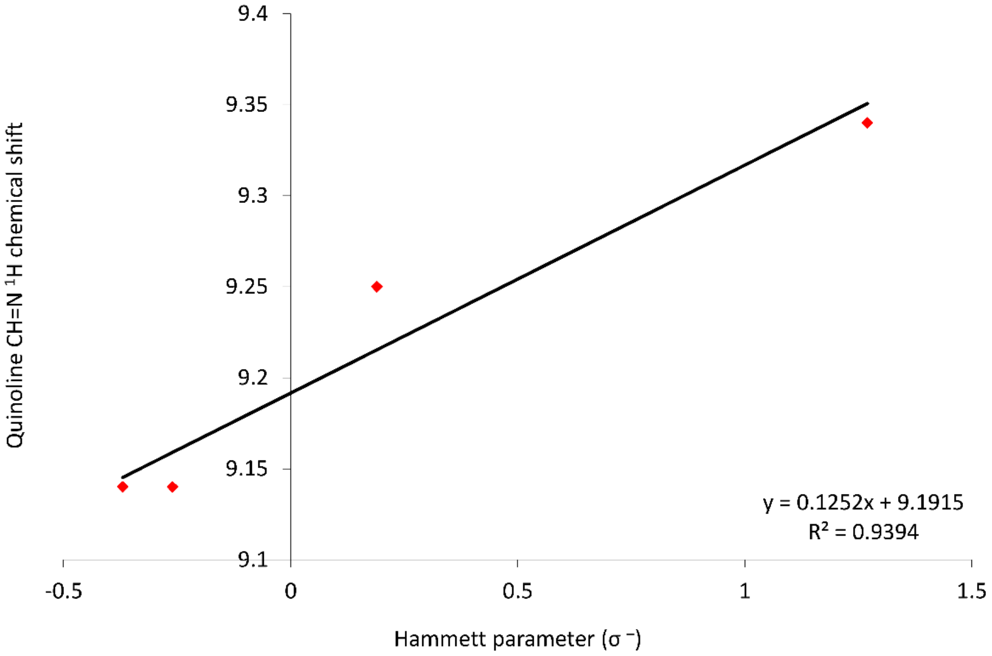

c)

Hammett plots of pyridine CH=N ^{1}H NMR shift of compounds **3–6** as a function of a) σ, b) σ$^+$ and c) σ$^-$.

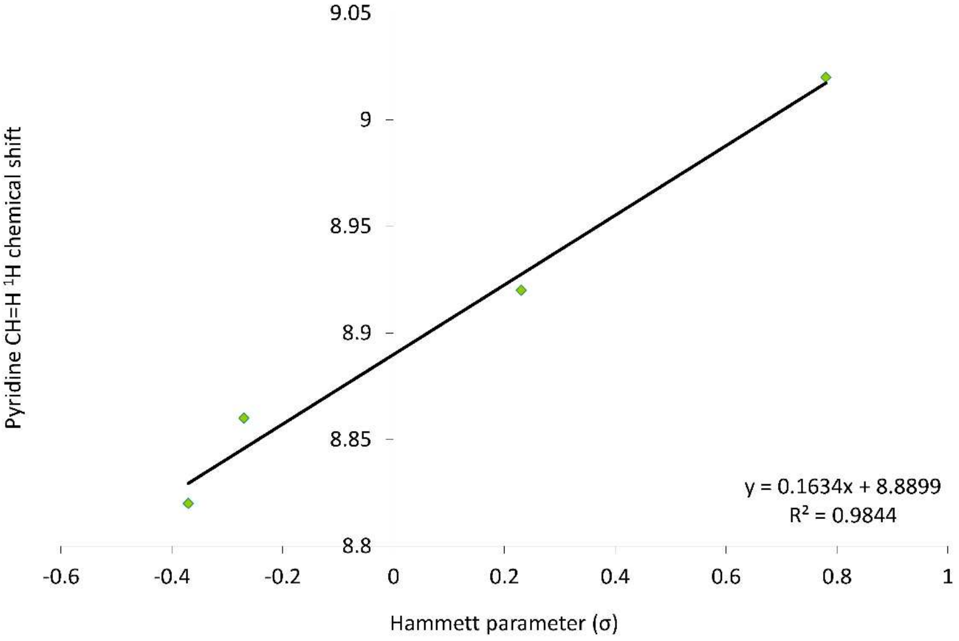

a)

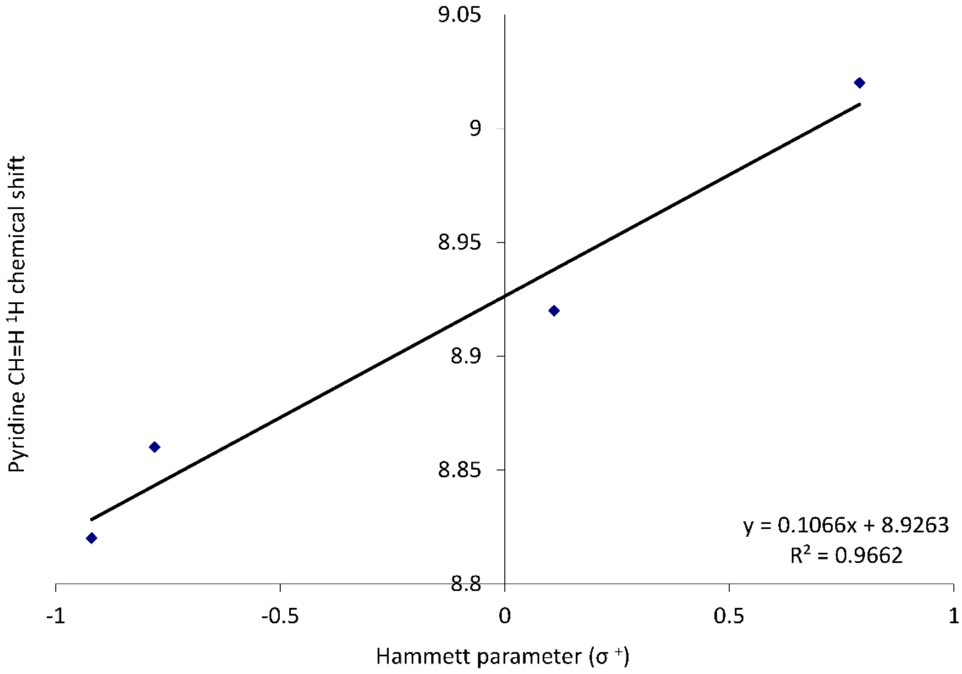

b)

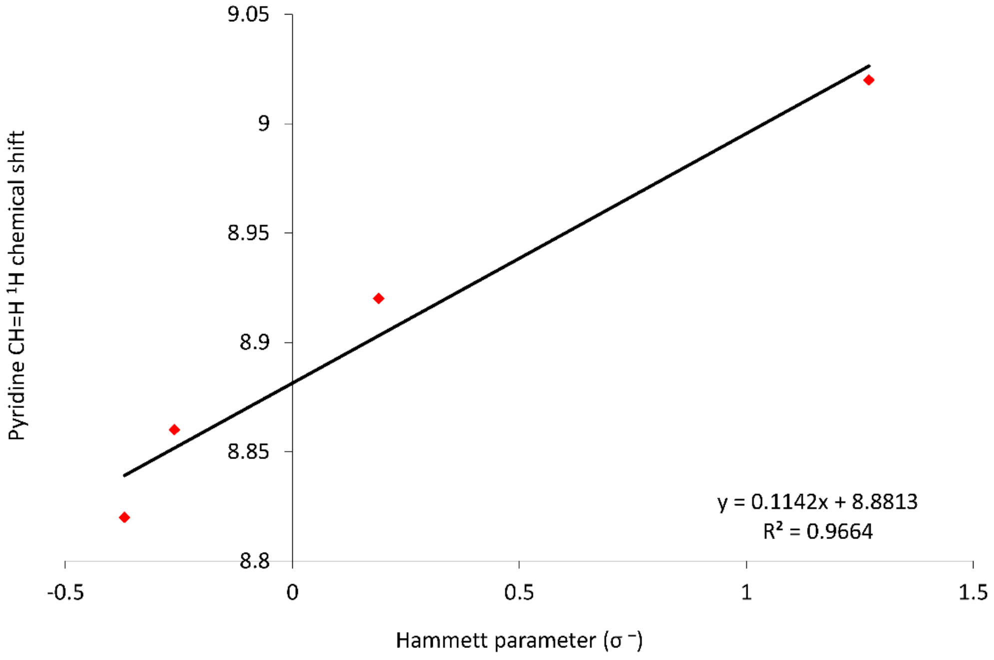

c)

Hammett plots of pyridine CH=N ^{1}H NMR shift of compounds **7–10** as a function of a) σ, b) σ^+ and c) σ^-.

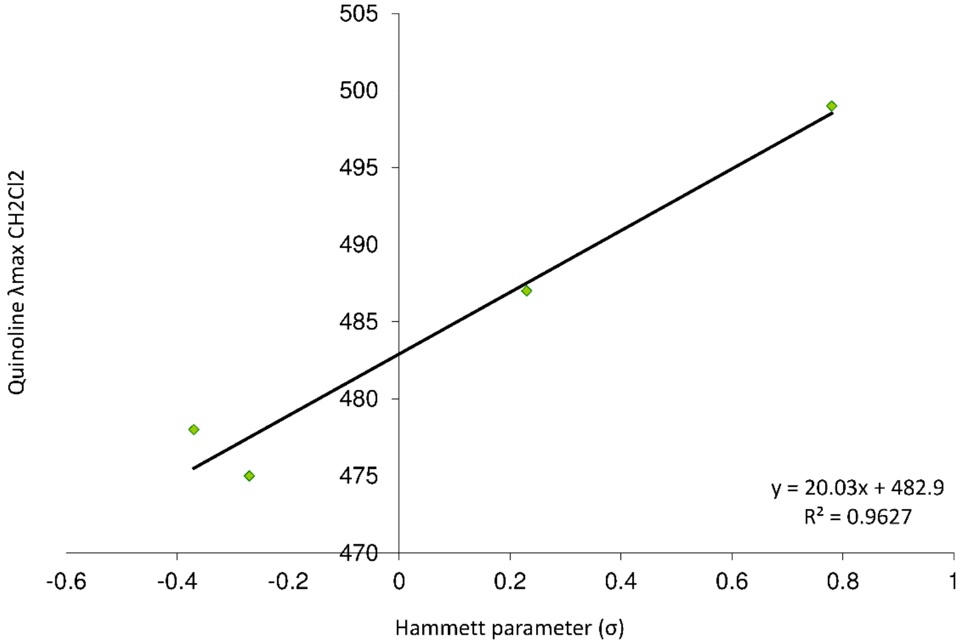
505
500
495
490
485
480
475
470
-0.6
-0.4
-0.2
0
0.2
0.4
0.6
0.8
1
Quinoline λmax CH2Cl2
Hammett parameter (σ)
y = 20.03x + 482.9
R² = 0.9627

a)

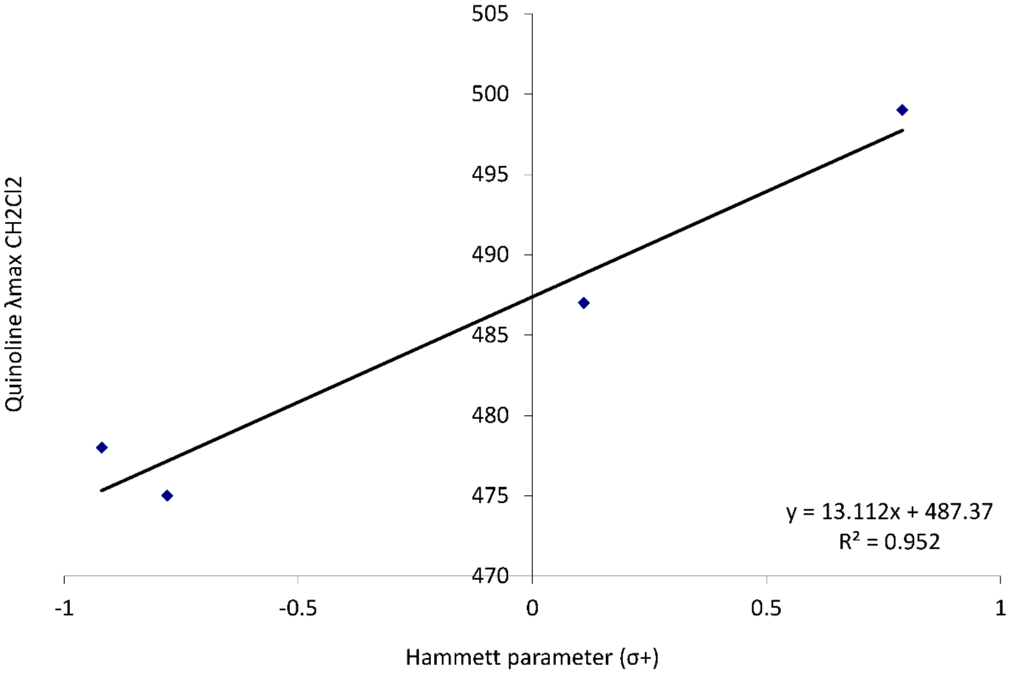
505
500
495
490
485
480
475
470
-1
-0.5
0
0.5
1
Quinoline λmax CH2Cl2
Hammett parameter (σ+)
y = 13.112x + 487.37
R² = 0.952

b)

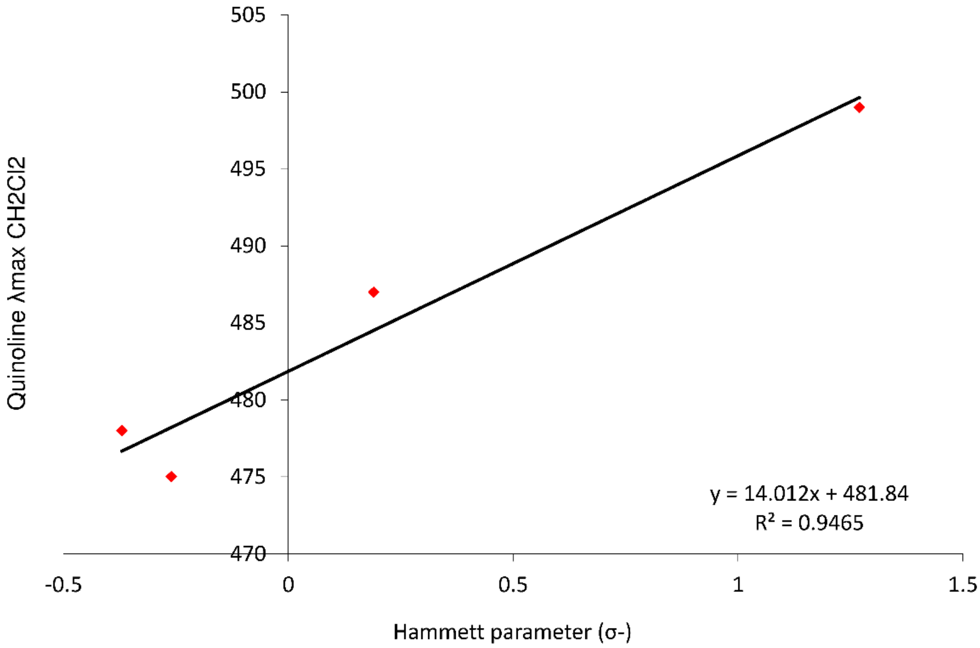

c)

Hammett plots of quinoline λ_{max} of compounds **3–6,** recorded in dichloromethane**,** as a function of a) σ, b) σ^{+} and c) σ^{-}.

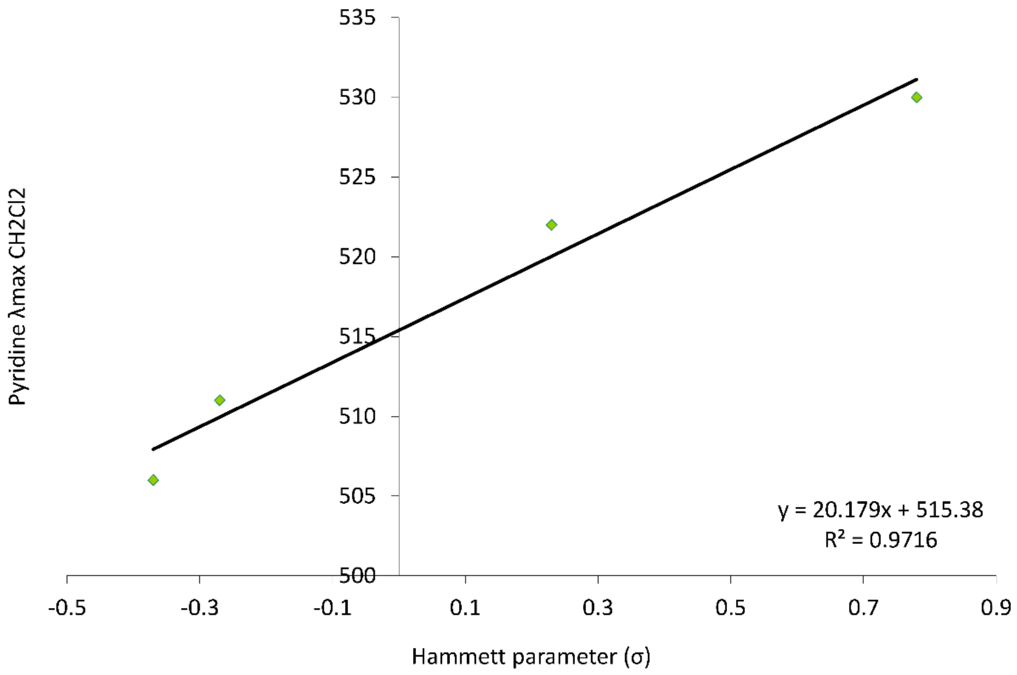
535
530
525
520
515
510
505
500
-0.5
-0.3
-0.1
0.1
0.3
0.5
0.7
0.9
Pyridine λmax CH2Cl2
Hammett parameter (σ)
y = 20.179x + 515.38
R² = 0.9716

a)

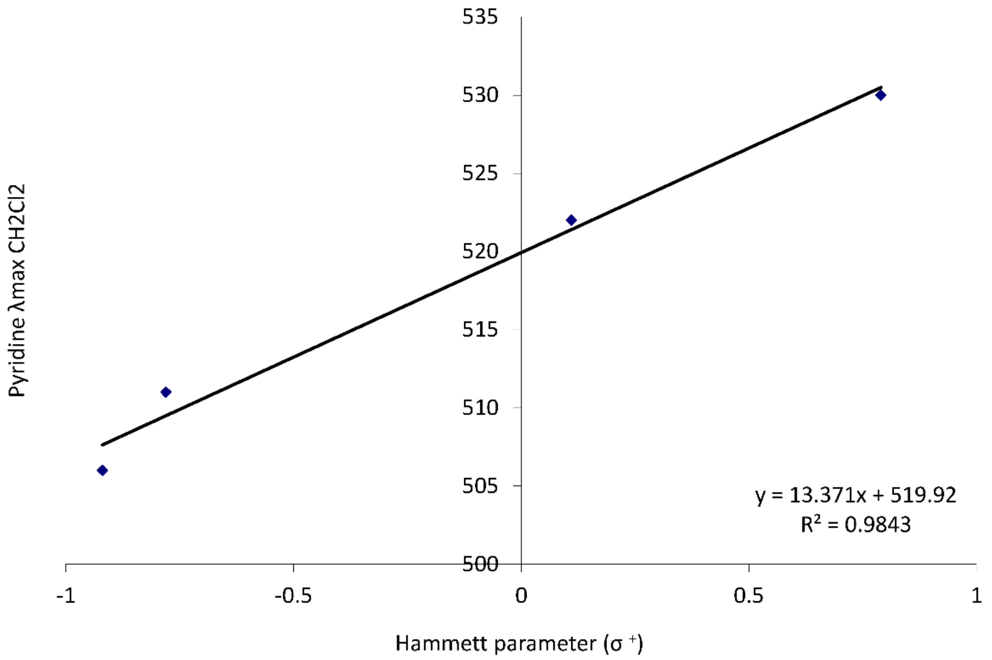
535
530
525
520
515
510
505
500
-1
-0.5
0
0.5
1
Pyridine λmax CH2Cl2
Hammett parameter (σ ⁺)
y = 13.371x + 519.92
R² = 0.9843

b)

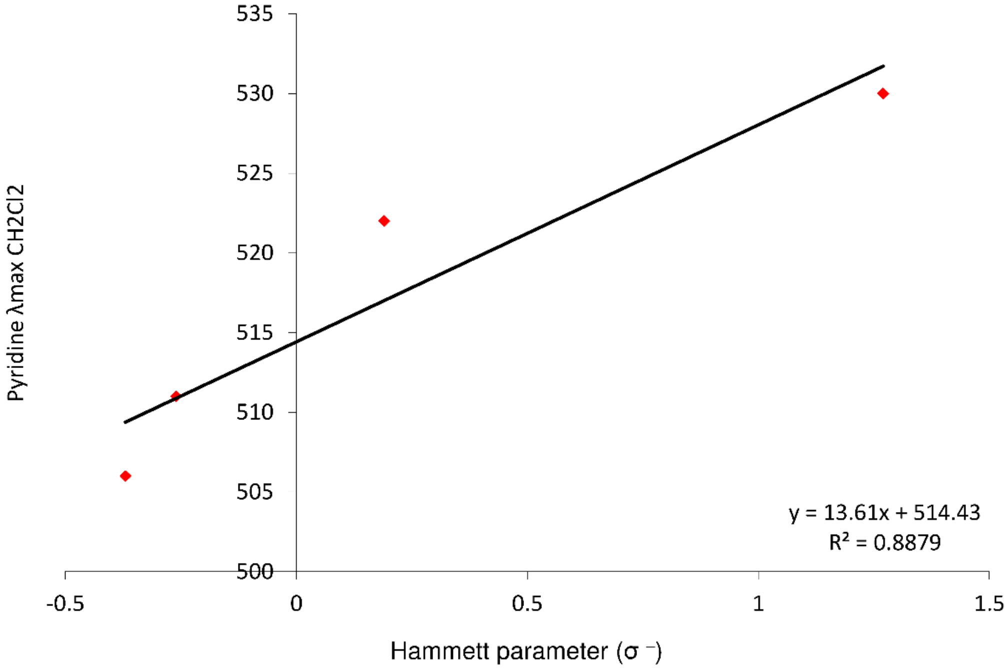

c)

Hammett plots of quinoline λ_{max} of compounds **7–10,** recorded in dichloromethane**,** as a function of a) σ, b) σ^+ and c) σ^-.